

General Materials Science

Byungwoo Park

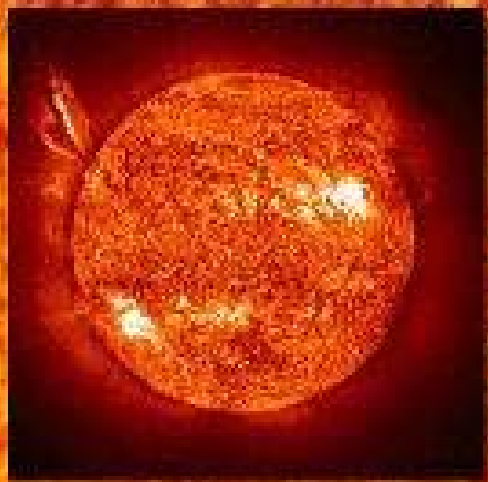
**Department of Materials Science and Engineering
Seoul National University**

<http://bp.snu.ac.kr>

Earth shown
for size comparison



Google Earth



Nanoscale Control: Nanomaterials for Energy

White LED



PDP



Cellular Phone



MP3



Phosphor

Fuel Cell

Nanomaterials
for
Energy

Solar Cell

Li⁺ Battery



Solar Panel



Portable Devices



Laptop



PMP

Global Warming: How to Win?



TIME (2008)

Hard Times: The End of Prosperity?

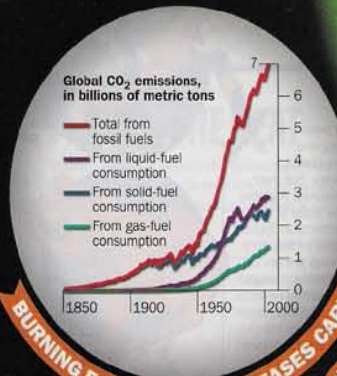


TIME (2008)

VICIOUS CYCLES

The debate over whether Earth is warming up is over. Now we're learning that climate disruptions feed off one another in accelerating spirals of destruction. Scientists fear we may be approaching the point of no return

TIME graphic by Joe Lertola; reported by Missy Adams



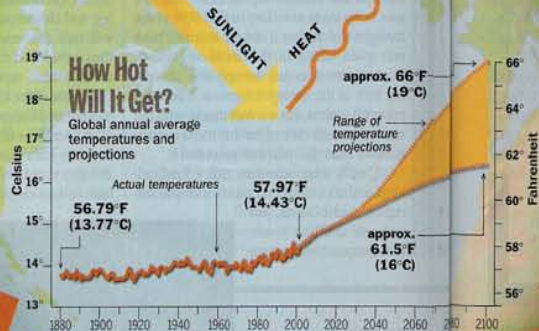
FUELING THE FIRE The amount of carbon dioxide in the atmosphere is climbing fast. Most of it comes from burning fuels for energy—gasoline in cars or coal for electricity, for example. The U.S., with less than 5% of the world's population, produces one-quarter of all greenhouse gases

SPREADING THE PAIN Deforestation through clear-cutting or burning sows havoc far beyond the affected area. The fires release still more carbon into the atmosphere, fewer plants survive to convert CO₂ into oxygen, and scorched soil absorbs more heat and retains less water, increasing droughts

THE GREENHOUSE EFFECT

Without the greenhouse effect, life on Earth would not be possible. Energy from the sun is absorbed by the planet and radiated back out as heat. Atmospheric gases like carbon dioxide trap that heat and keep it from leaking into space. That's what keeps us warm at night.

But as humans pour ever increasing amounts of greenhouse gases into the atmosphere, more of the sun's heat gets trapped, and the planet gets a fever



BURNING FORESTS Plants take in CO₂. Fires release carbon. Less carbon absorbed. Soil dries out.



REDUCES OXYGEN AND INCREASES DROUGHT



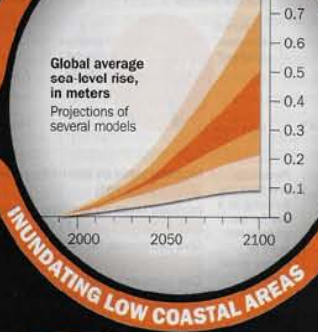
RIISING TEMPERATURES
MELT POLAR ICE AND PERMAFROST

THAWING OUT The North Pole may be seasonally ice free by 2050. Melting permafrost will release vast amounts of trapped carbon into the air

Near-surface permafrost
1980-99 (blue), 2080-99 (est.) (red)

WASHING ASHORE The ice at the North Pole is floating, so as it melts, the sea level won't change much. But the massive ice sheets over Antarctica and Greenland are another story. If both melted completely, sea levels could rise nearly 220 ft. (72 m). That's a worst-case scenario. But the melting is accelerating, and sea levels are projected to rise gradually, threatening low-lying communities

MELTING ICE RAISES SEA LEVELS



INUNDATING LOW COASTAL AREAS



LESS ICE MEANS MORE HEAT
WHICH MEANS LESS ICE

SPEEDING UP Ice reflects nearly all the sun's energy that hits it. As the planet's ice melts, more of that energy is absorbed by Earth—which further raises the temperature. That, in turn, makes the remaining ice melt quicker

cold water, so it floats on the surface. As it reaches Europe and releases its heat, the current grows denser and sinks, flowing back to the south and crossing under the northbound Gulf Stream until it reaches the tropics and starts to warm again. The cycle works splendidly, provided the water remains salty enough. But if it becomes diluted by freshwater, the salt concentration drops, and the water gets lighter, idling on top and stalling the current. Last December, researchers associated with Britain's National Oceanography Center reported that one component of the system that drives the Gulf Stream has slowed about 30% since 1957. It's the increased release of Arctic and Greenland meltwater that appears to be causing the problem, introducing a gush of freshwater that's overwhelming the natural cycle. In a global-warming world, it's unlikely that any amount of cooling that resulted from this would be sufficient to support glaciers, but it could make things awfully uncomfortable.

"The big worry is that the whole climate of Europe will change," says Adrian Luckman, senior lecturer in geography at the University of Wales, Swansea. "We in the U.K. are on the same latitude as Alaska. The reason we can live here is the Gulf Stream."

DROUGHT
AS FAST AS GLOBAL WARMING IS TRANSFORMING the oceans and the ice caps, it's having an even more immediate effect on land. People, animals and plants living in dry, mountainous regions like the western U.S. make it through summer thanks to snowpack that collects on peaks all winter and slowly melts off in warm months. Lately the early arrival of spring and the unusually blistering summers have caused the snowpack to melt too early, so that by the time it's needed, it's largely gone. Climatologist Philip Mote of the University of Washington has compared decades of snowpack levels in Washington, Oregon and California and found that they are a fraction of what they were in the 1940s, and some snowpaks have vanished entirely.

Global warming is tipping other regions of the world into drought in different ways. Higher temperatures bake moisture out of soil faster, causing dry regions that live at the margins to cross the line into full-blown crisis. Meanwhile, El Niño events—the warm pooling of Pacific waters that periodically drives worldwide climate patterns and has been occurring more frequently in global-warming years—further inhibit precipitation

Source: Intergovernmental Panel on Climate Change, Third Assessment Report; NOAA; NASA's National Snow and Ice Data Center; Carbon Dioxide Information Analysis Center; National Center for Atmospheric Research; U.S. Global Change Research Program; Goddard Institute for Space Studies

More and more
land is being
devastated by drought...

MOONSCAPE Cattle struggle across parched land in Ethiopia. The amount of the earth's surface afflicted by drought has more than doubled since the 1970s

BOBBY HAAS—NATIONAL GEOGRAPHIC IMAGE COLLECTION

GLOBAL WARMING



Polar ice caps
are melting faster
than ever...

AT SEA In the Canadian high Arctic, a polar bear negotiates what was once solid ice. Bears are drowning as warmer waters widen the distance from floe to floe
ARCTICNET—ACE

PHYSICS TODAY

APRIL 2002

EARTH AT NIGHT: composite satellite image

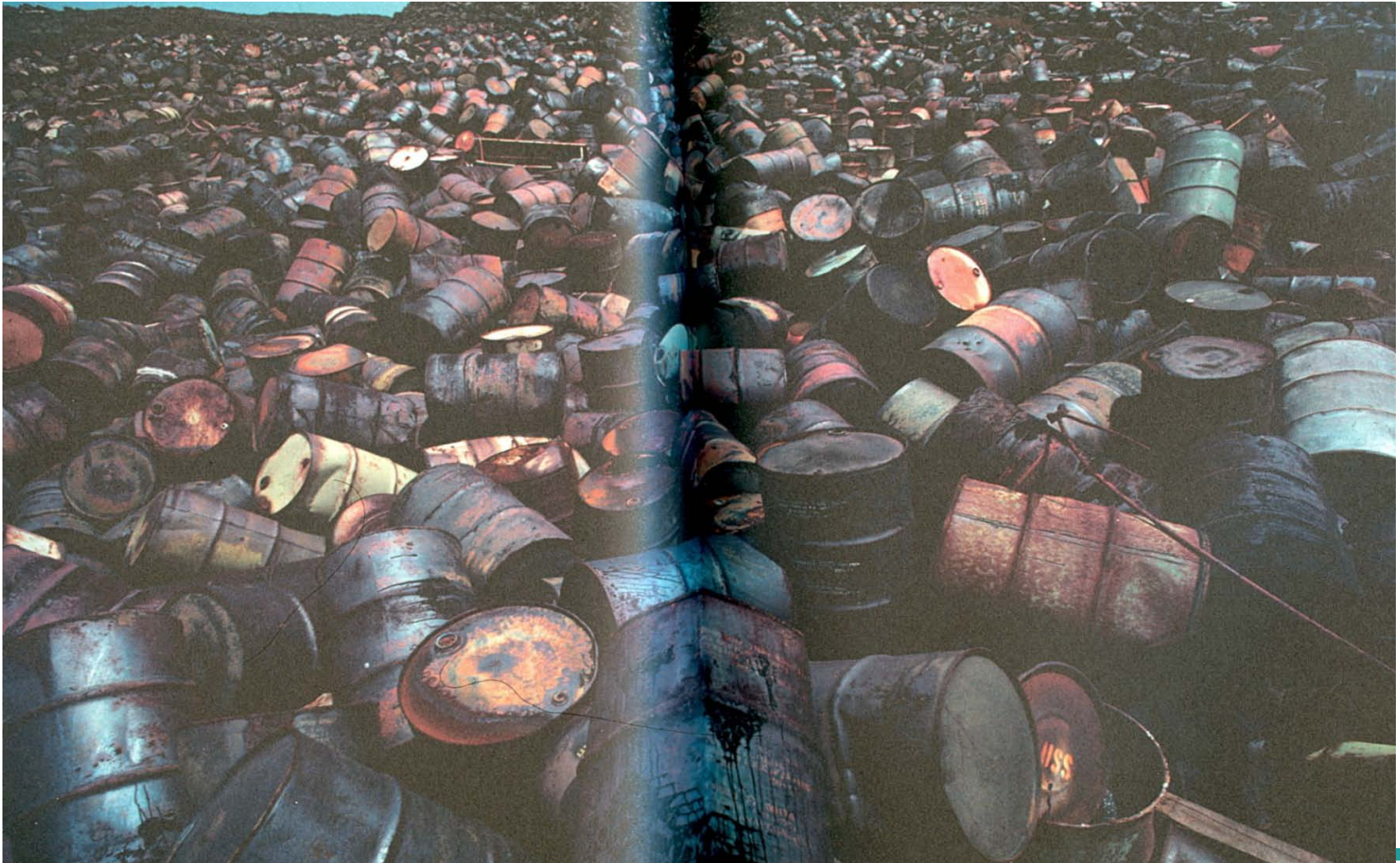


SPECIAL ISSUE: THE ENERGY CHALLENGE

Ascension Island (1970~1990)

百年の愚行 (ONE HUNDRED YEARS OF IDIOCY), 2002

Tetsuya Ozaki



U.S. / San Francisco (1989)



百年の愚行 (ONE HUNDRED YEARS OF IDIOCY), 2002

Argentina / Buenos Aires (1993)



百年の愚行 (ONE HUNDRED YEARS OF IDIOCY), 2002

Philippine / Lubango (1996)



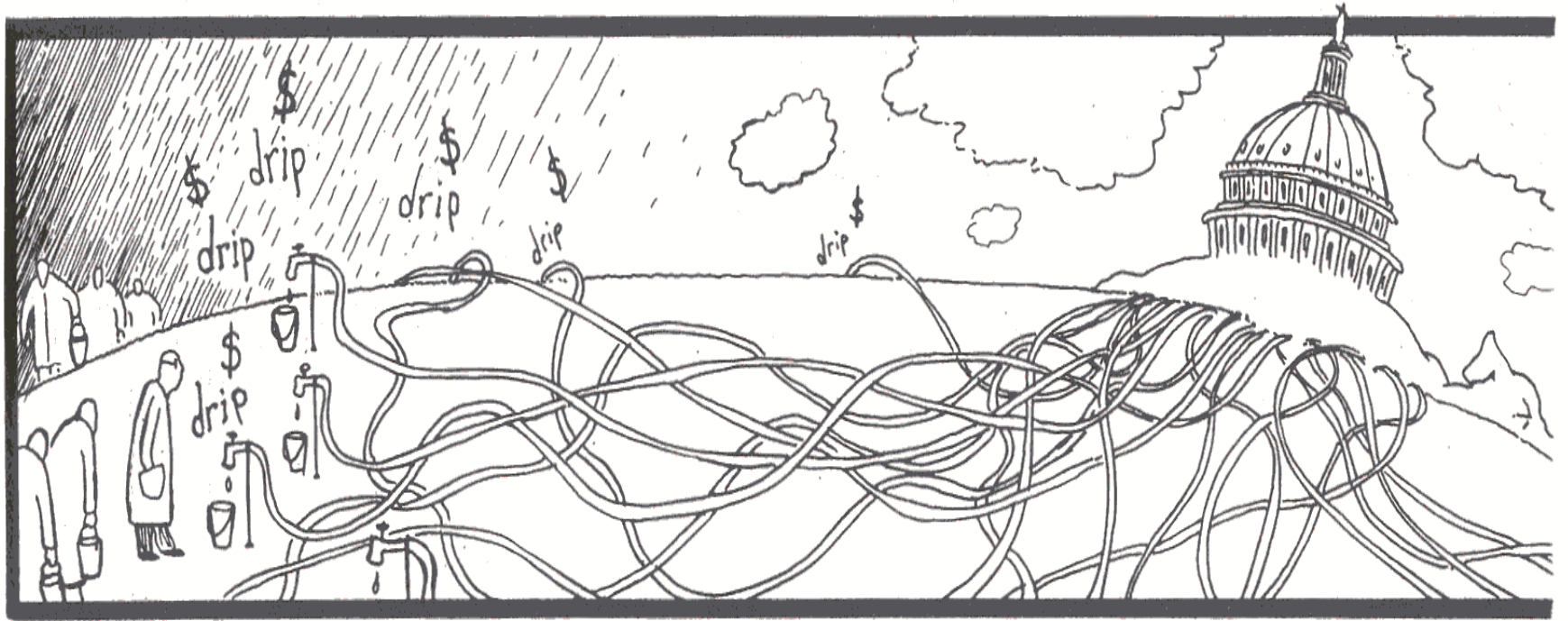
百年の愚行 (ONE HUNDRED YEARS OF IDIOCY), 2002

Zaire / Goma (1994)

cholera

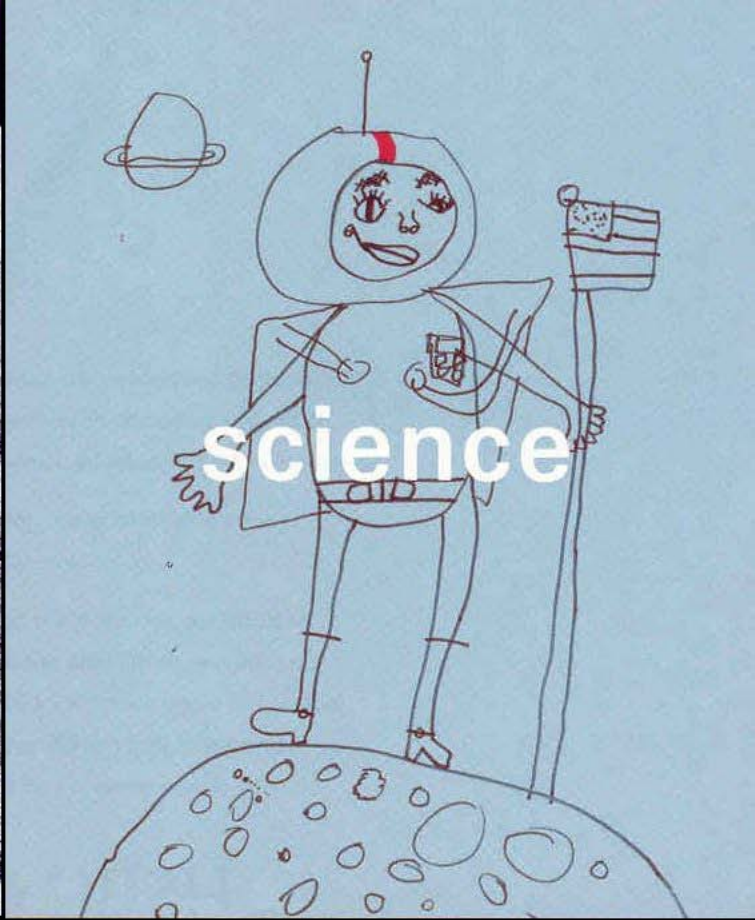


百年の愚行 (ONE HUNDRED YEARS OF IDIOCY), 2002

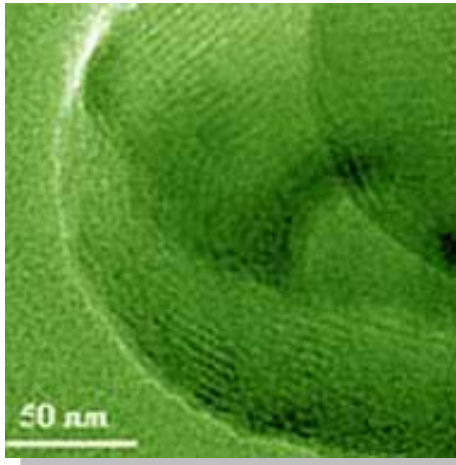


PAUL DWYER

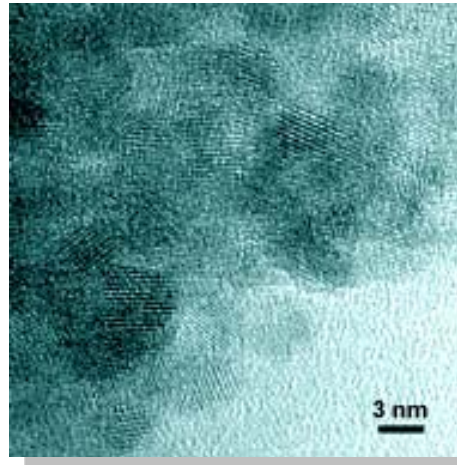
Science vs. Art



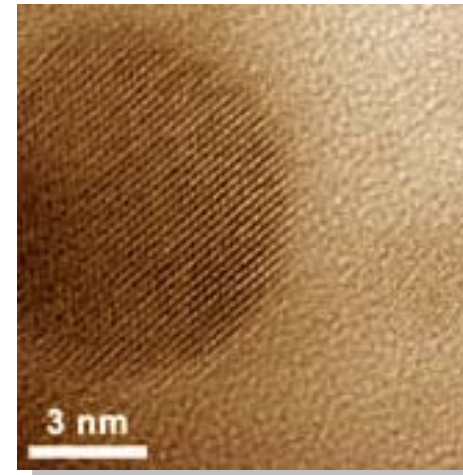
Synthesis/Control of Nanostructures for Desirable Applications



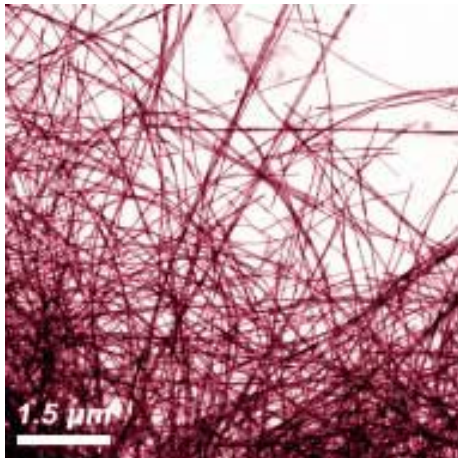
Mesoporous Structure



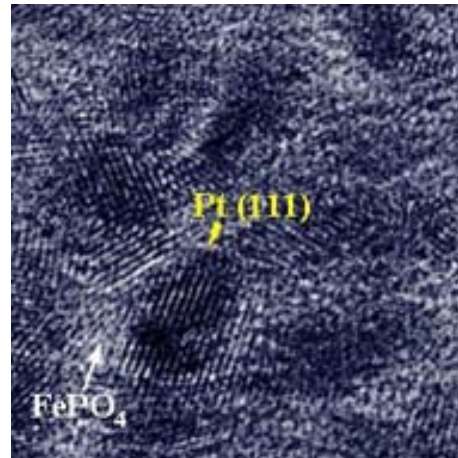
Oxide Nanoparticles



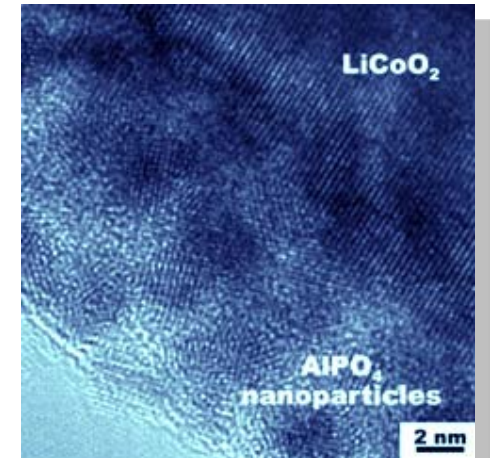
Semiconductor Nanoparticles



Nanowires

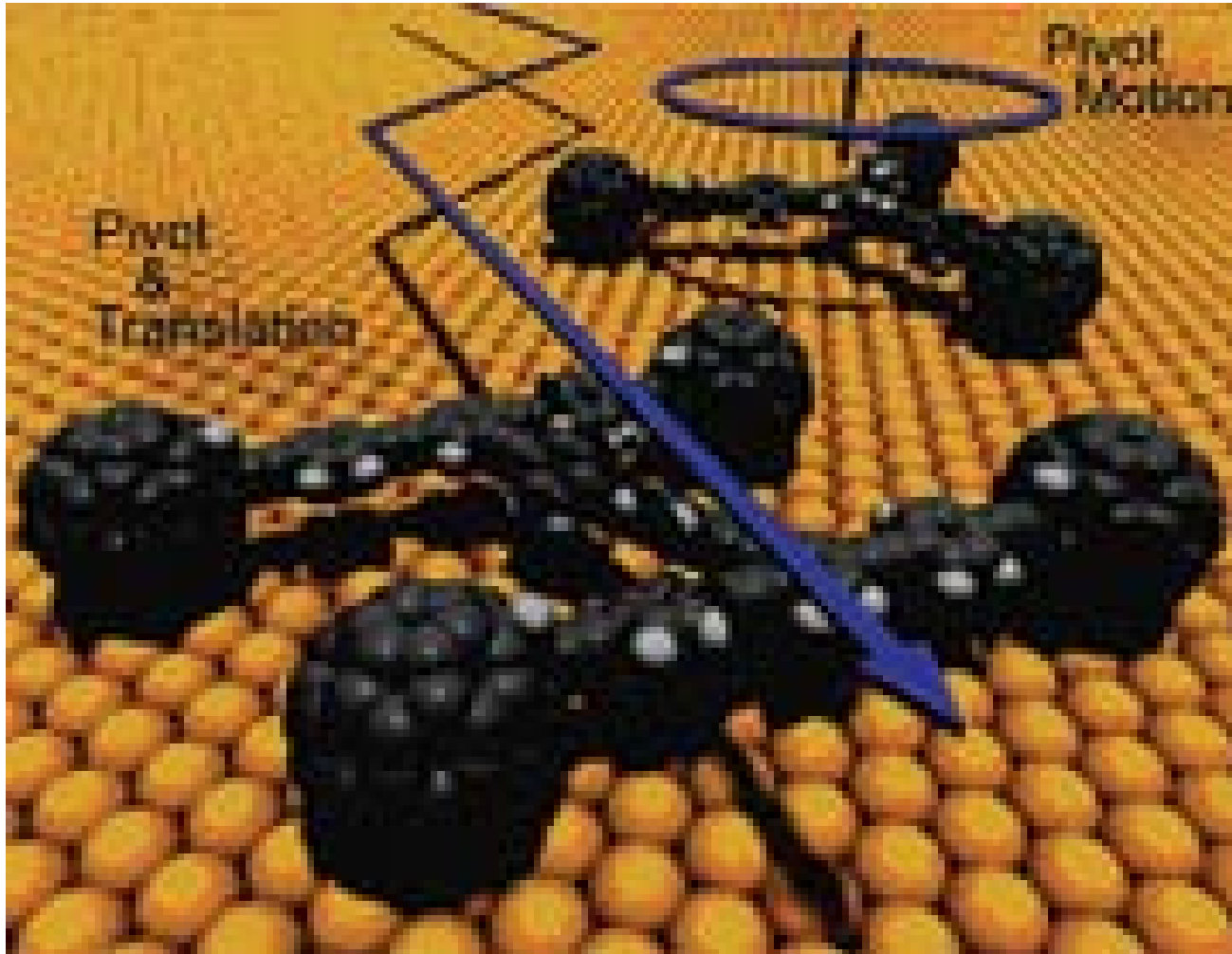


Nanocomposites

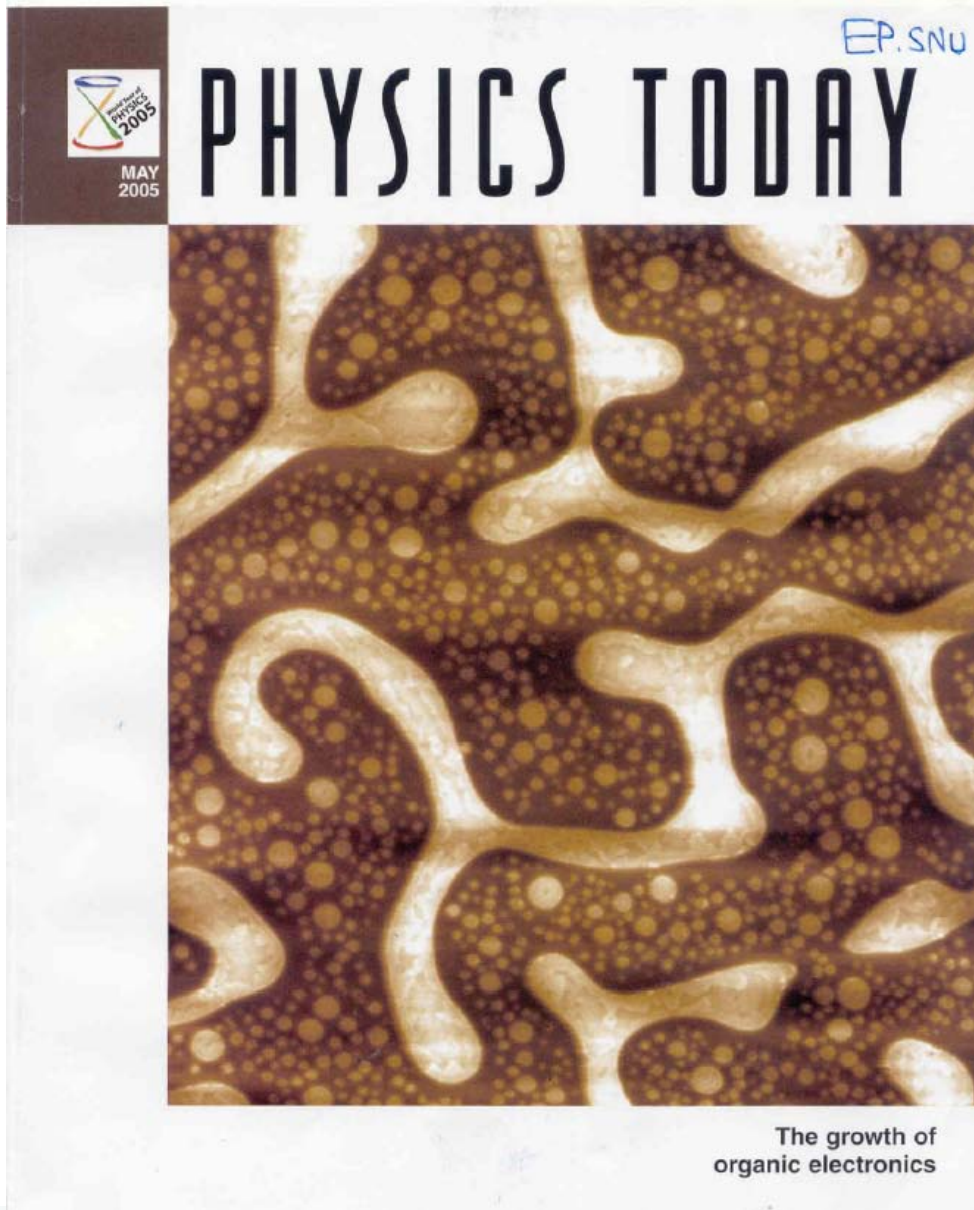


Nanoscale Coating

A Nanoscale (Nanocar) Vehicle



*James M. Tour's Group
Rice University
Science 315, 1199 (2006)*



MRS BULLETIN

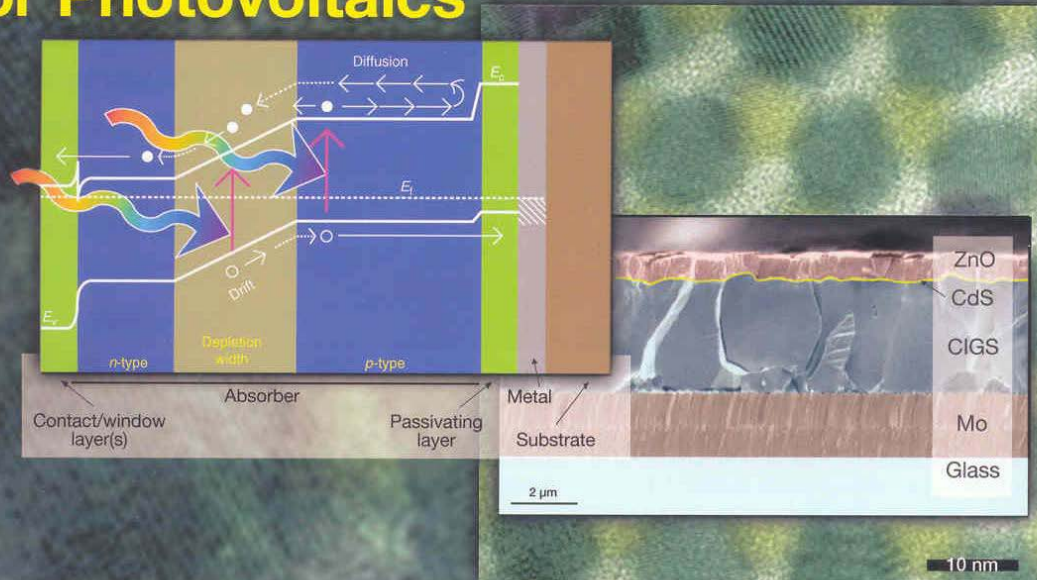
March 2007, Volume 32, No. 3

Serving the International
Materials Research Community

A Publication of the Materials Research Society



Advanced Inorganic Materials for Photovoltaics



Photovoltaic Conversion Efficiencies & Novel Conducting Polymers

Photovoltaic conversion efficiencies		
	Laboratory best*	Thermodynamic limit
Single junction		31%
Silicon (crystalline)	25%	
Silicon (nanocrystalline)	10%	
Gallium arsenide	25%	
Dye sensitized	10%	
Organic	3%	
Multijunction	32%	66%
Concentrated sunlight (single junction)	28%	41%
Carrier multiplication		42%

*As verified by the National Renewable Energy Laboratory. Organic cell efficiencies of up to 5% have been reported in the literature.

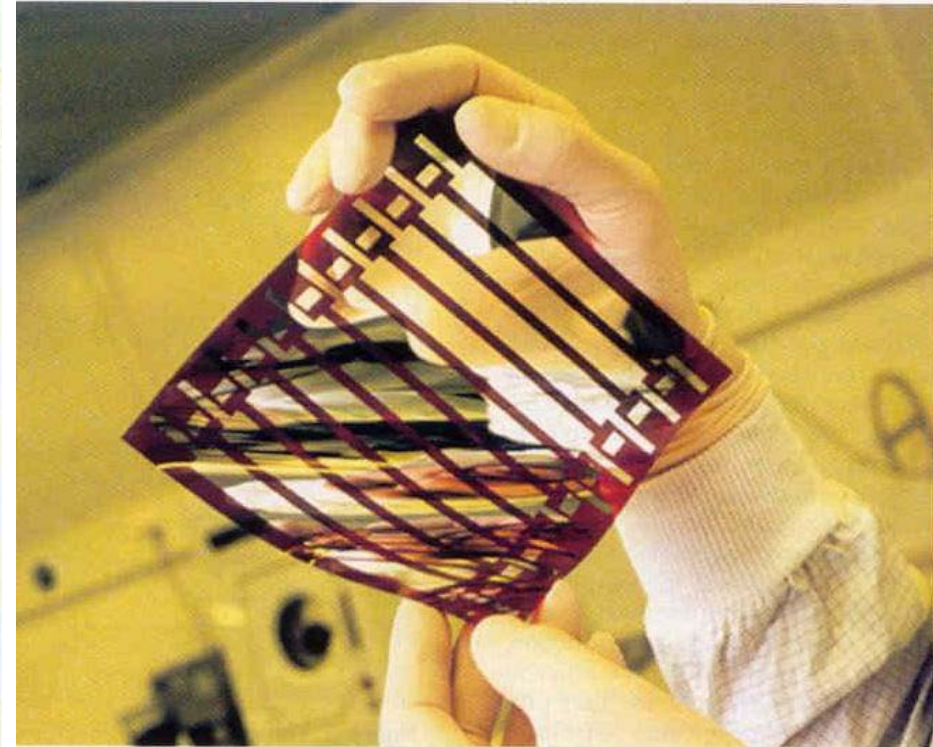
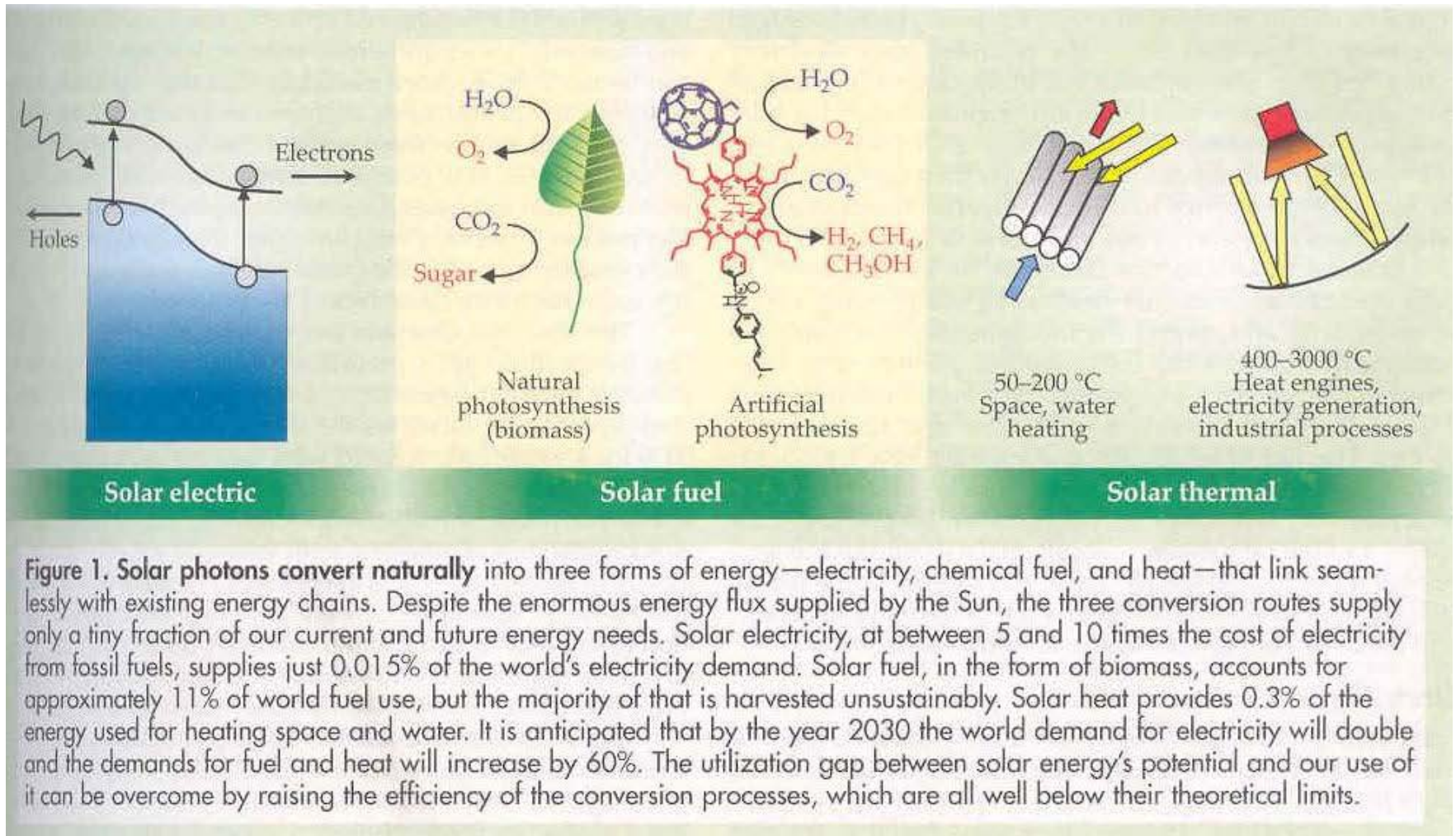


Figure 2. Novel conducting polymers enable solar cells that are flexible, inexpensive, and versatile. The new materials can be coated or printed onto flexible or rigid surfaces. (Image courtesy of Konarka Technologies.)

Physics Today (March 2007)

Solar Energy Conversion

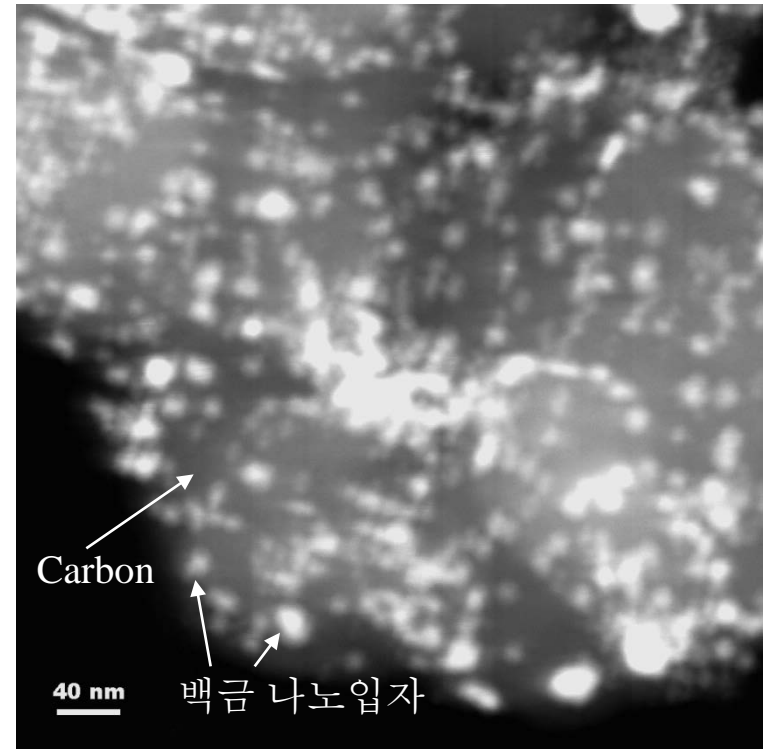


Physics Today (March 2007)
G. W. Crabtree and N. S. Lewis

Environment-Friendly Power Sources

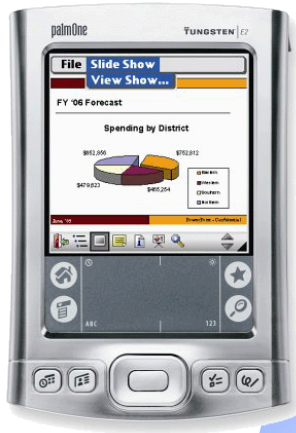


**Mobile
Electronics**



Hyundai Motors

High-Technology Electronics Equipments



PDA



**Laptop
Computer**



**Mobile
Phone**



**MP3
Player**

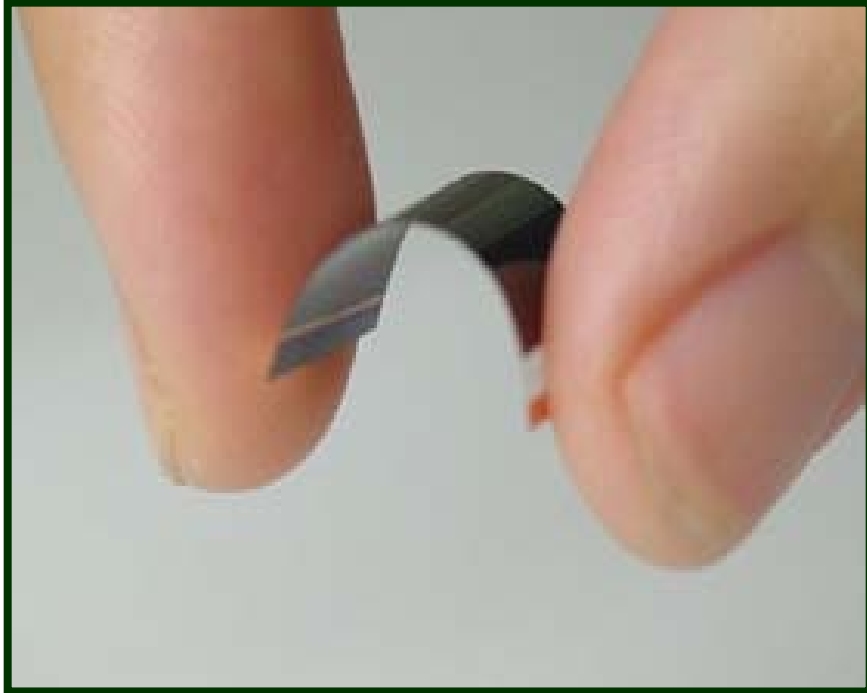


PMP



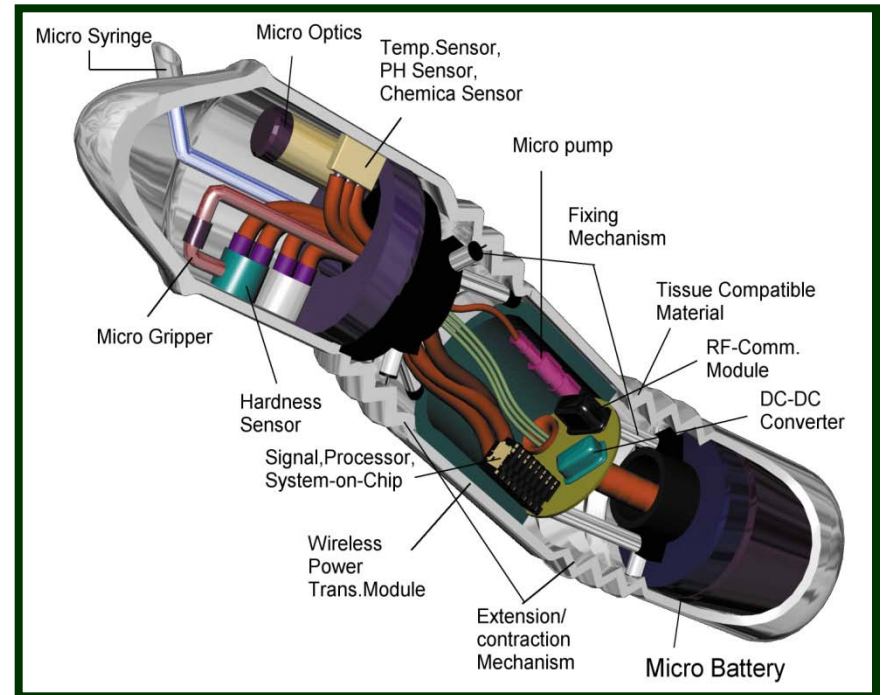
Digital Camera

Thin-Film Battery



- Smart Card
- Portable Sensors
- ID Tags
- SRAM

Capsule-Type Endoscope



- Sensors
- RF Communication

The Materials Science of Cosmetics -- Future ???



❖ What is a Scientific Paper?

A paper is not just an archival device for storing a completed research program. It is a structure for *planning* your research in progress.

❖ Why do I do the work?

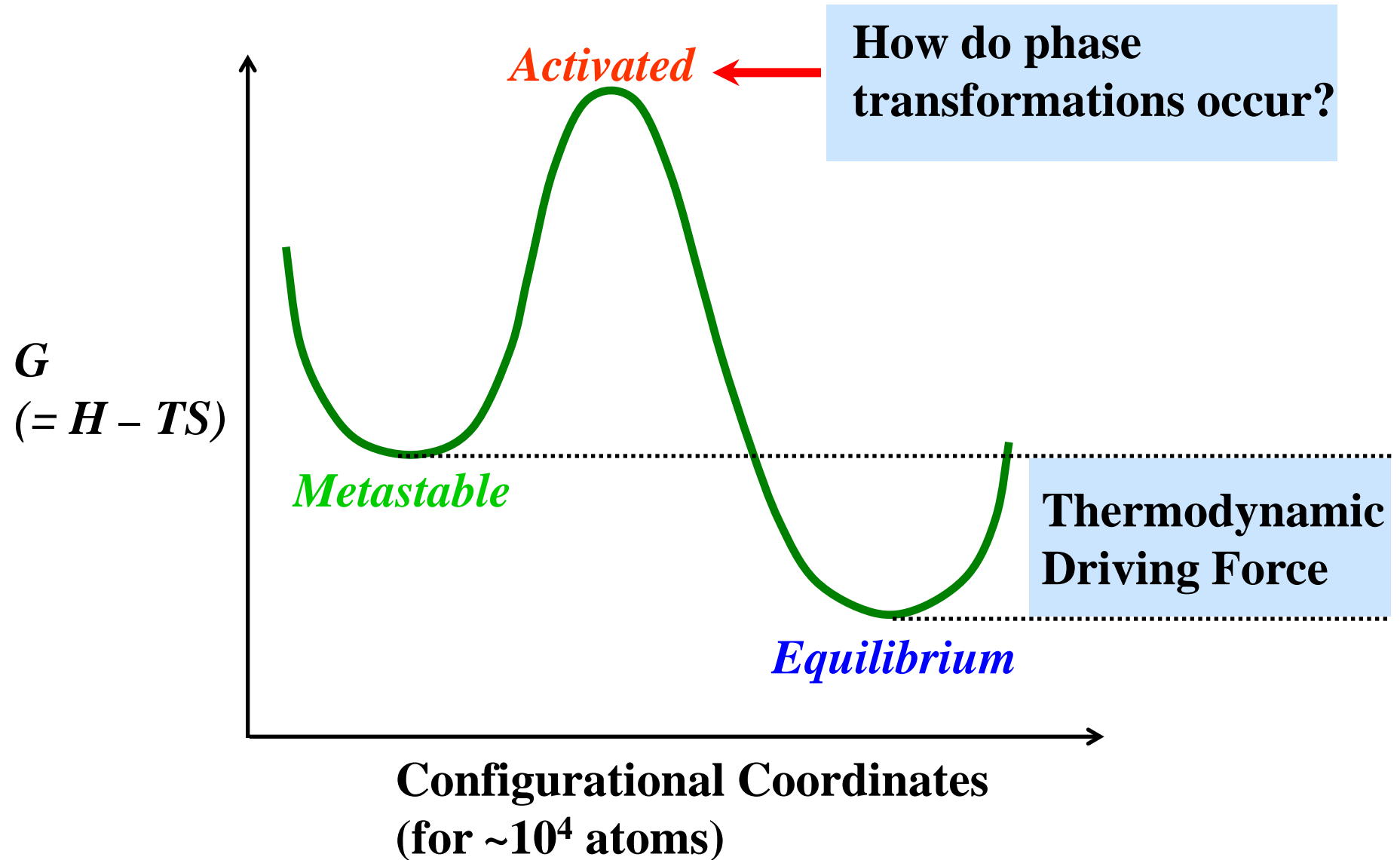
❖ What are the central motivations and hypothesis?

Prof. George M. Whitesides
Department of Chemistry and Chemical Biology
Harvard University
Cambridge, MA 02138 (U.S.A.)

Adv. Mater. (2004)

Thermodynamics = Why
Phase Transformations = How
Attractive Research

Phase Transformations of Nanomaterials

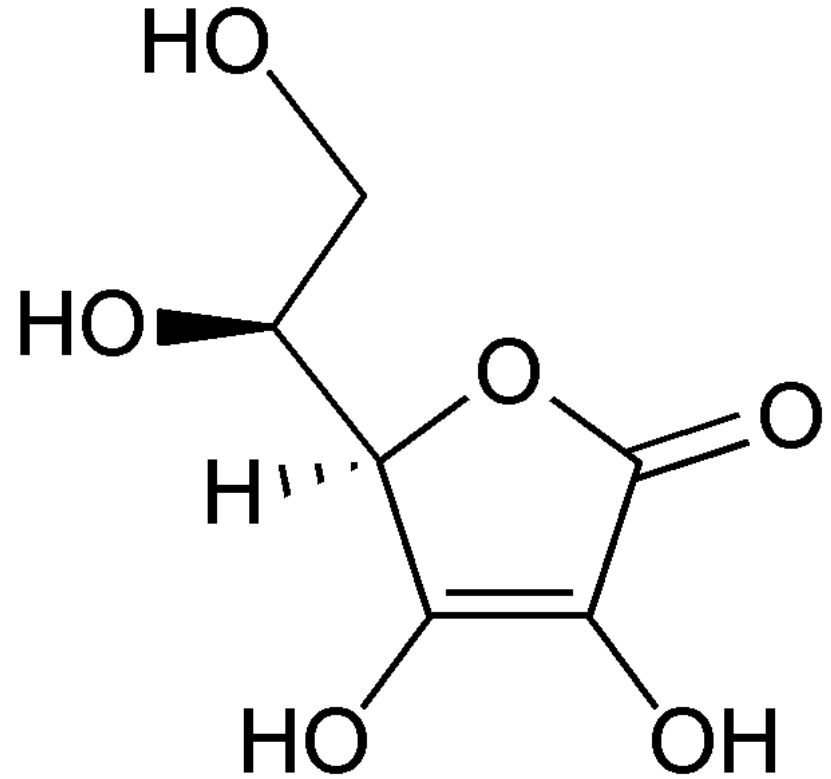
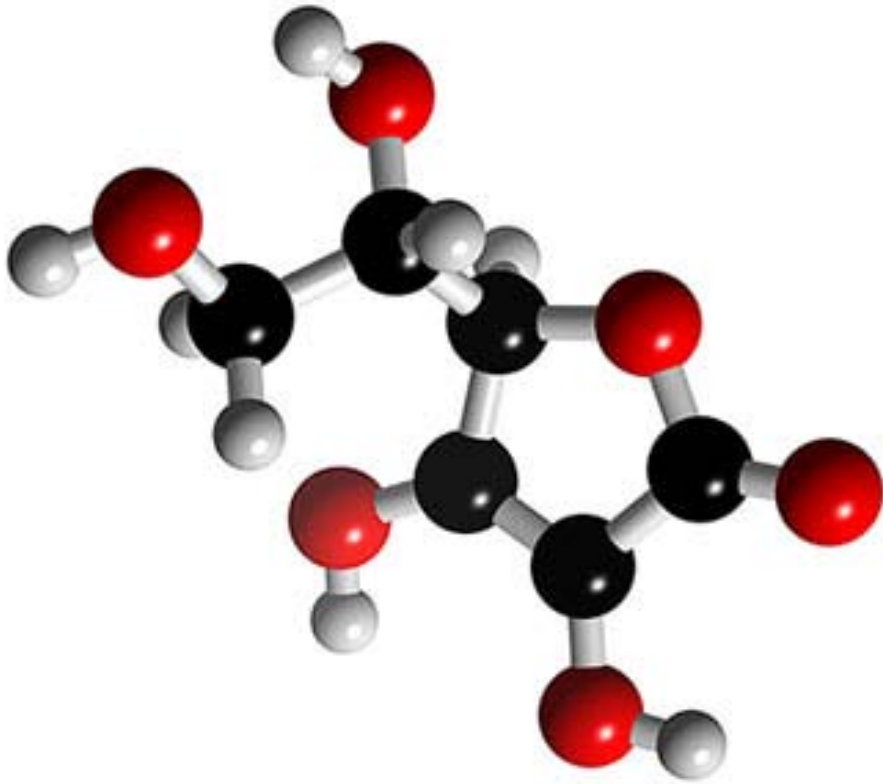




Prof. David Turnbull

Jeju Island (Aug. 2005)

Vitamin C



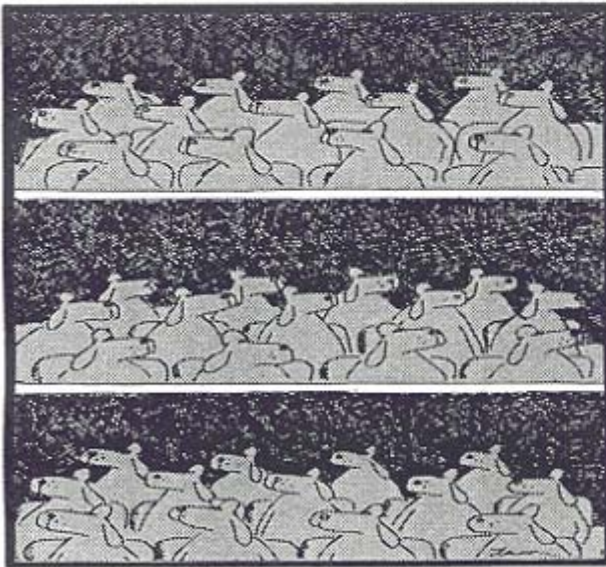
<http://www.3dchem.com/>

Gibbs Free Energy

Low Temperature
Enthalpy

$$H - TS$$

High Temperature
Entropy



At the popular dog film, *Man Throwing Slicks*



Characteristics of Phase Transformations

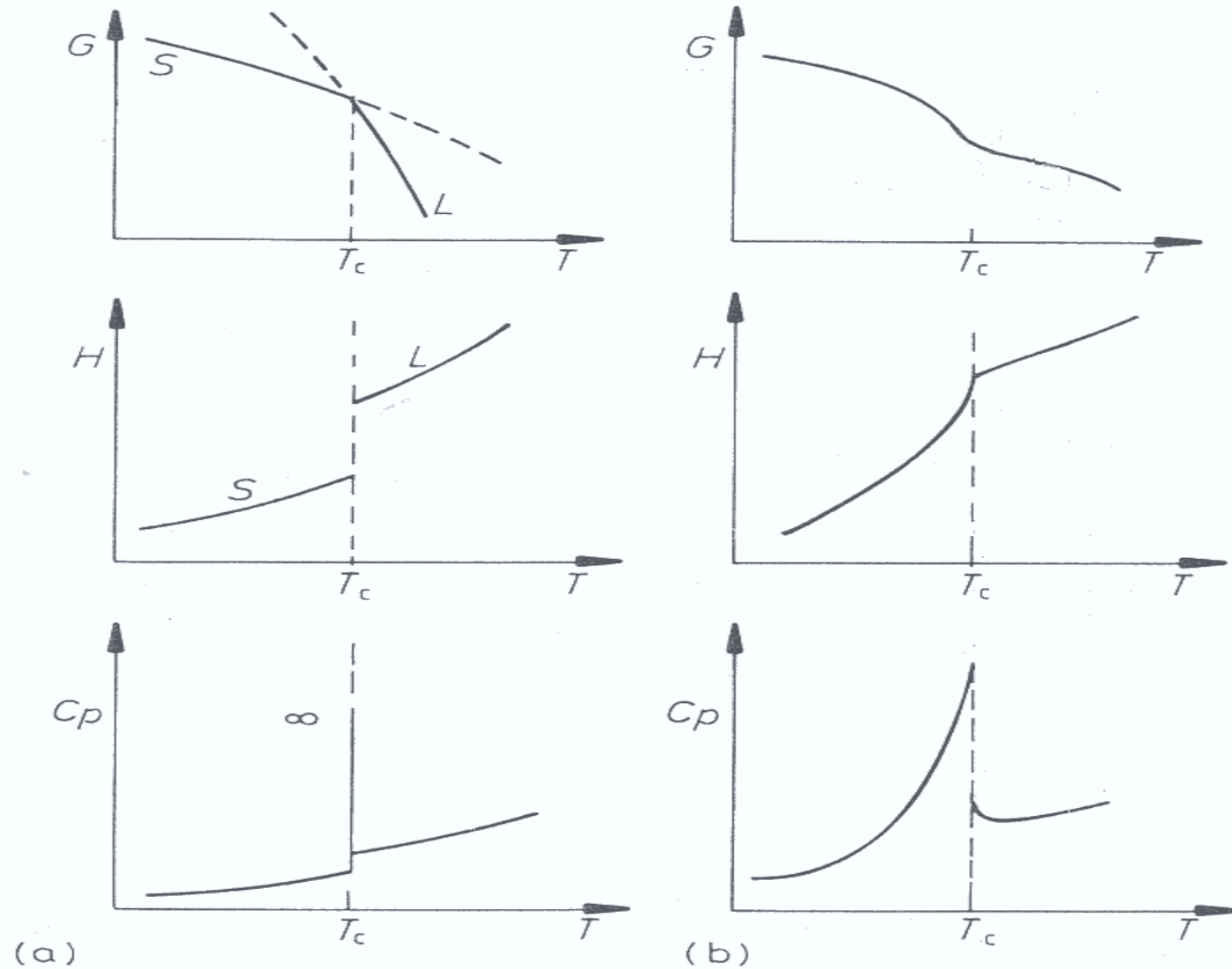


Fig. 5.82 The thermodynamic characteristics of (a) first-order and (b) second-order phase transformations.

First-Order Transition

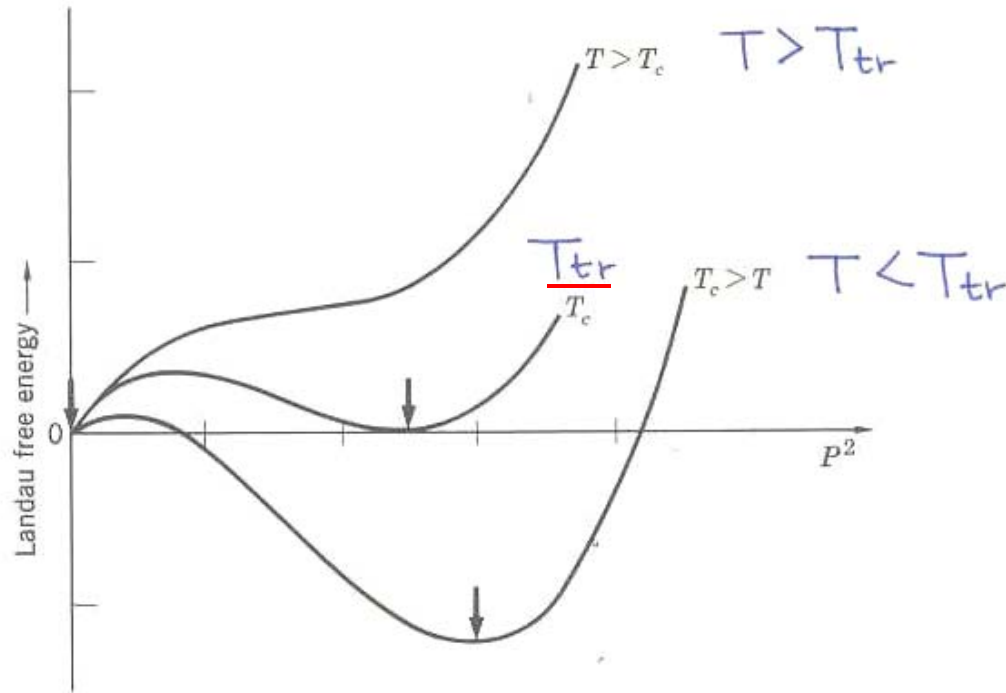


Figure 15 Landau free energy function versus (polarization)² in a first-order transition, at representative temperatures. At T_c the Landau function has equal minima at $P = 0$ and at a finite P as shown. For T below T_c the absolute minimum is at larger values of P ; as T passes through T_c there is a discontinuous change in the position of the absolute minimum. The arrows mark the minima.

¹⁵J. A. Gonzalo, Phys. Rev. **144**, 662 (1966); P. P. Craig, Phys. Letters **20**, 140 (1966).

Heat Capacity of Second-Order Transition

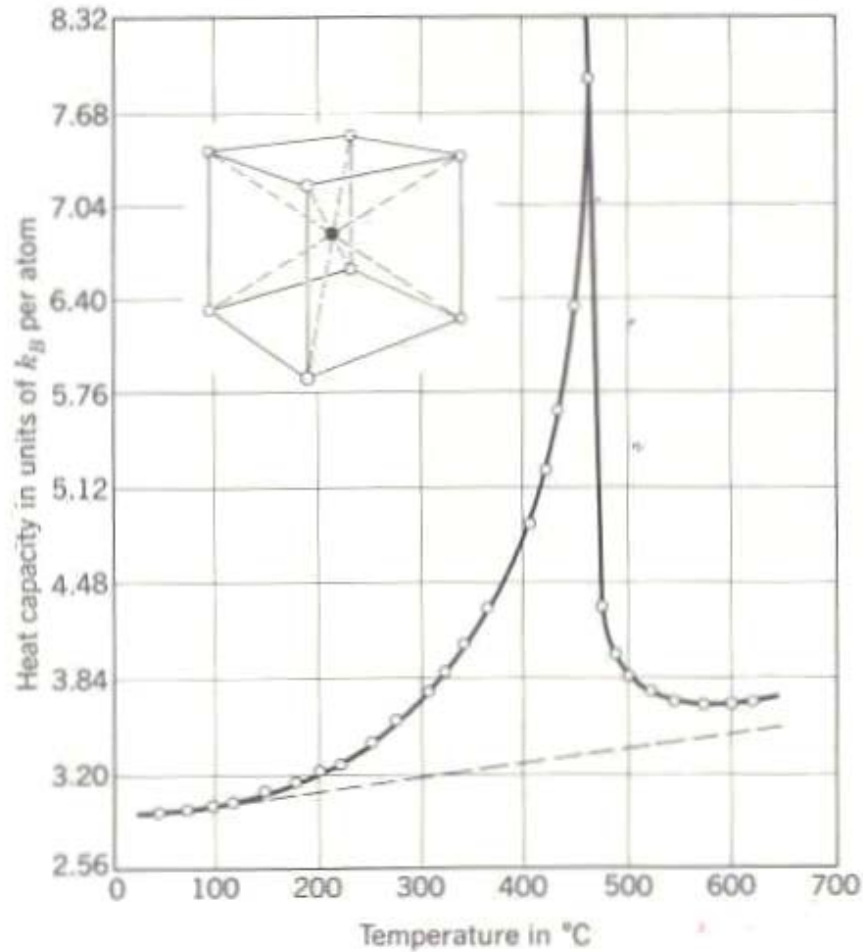
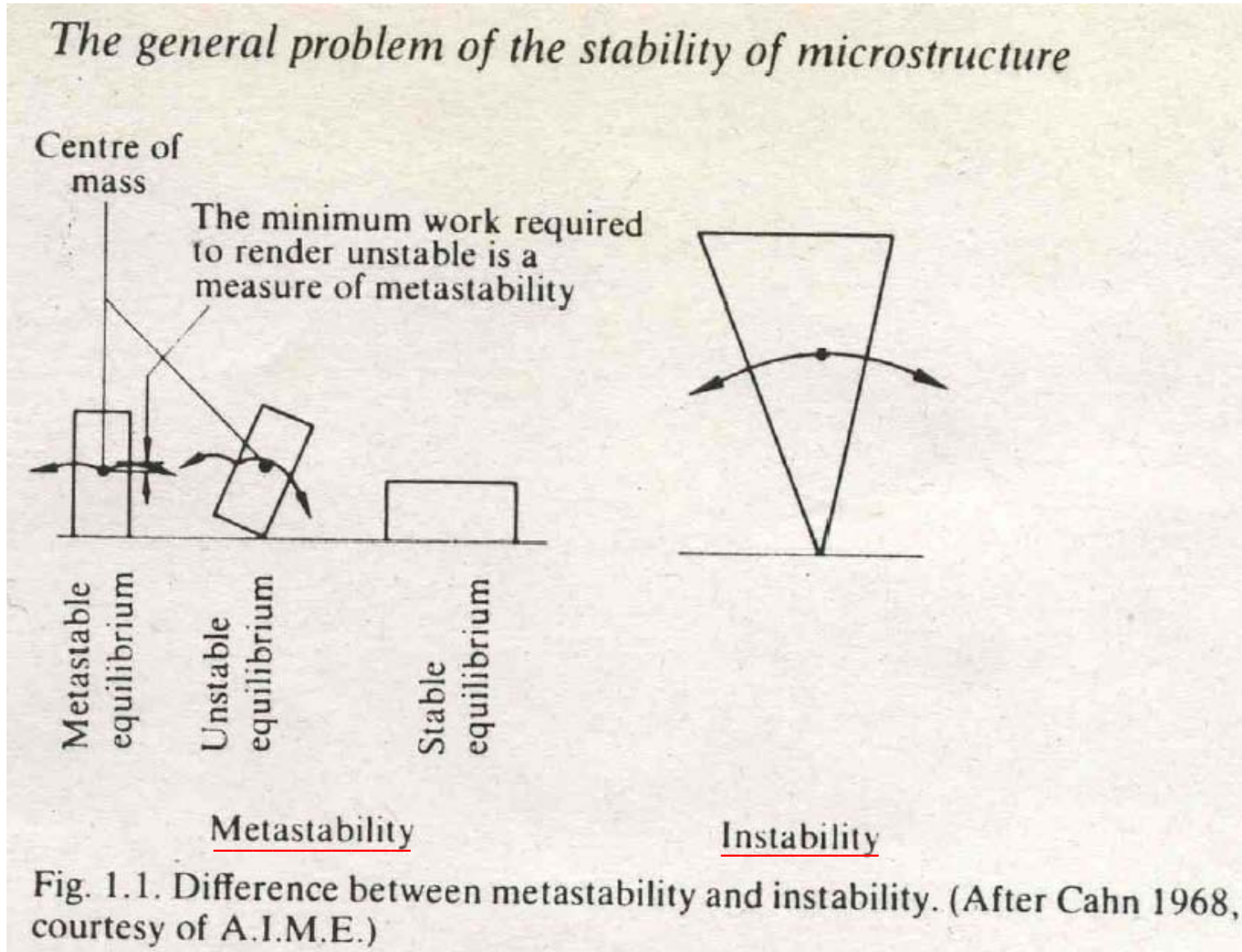
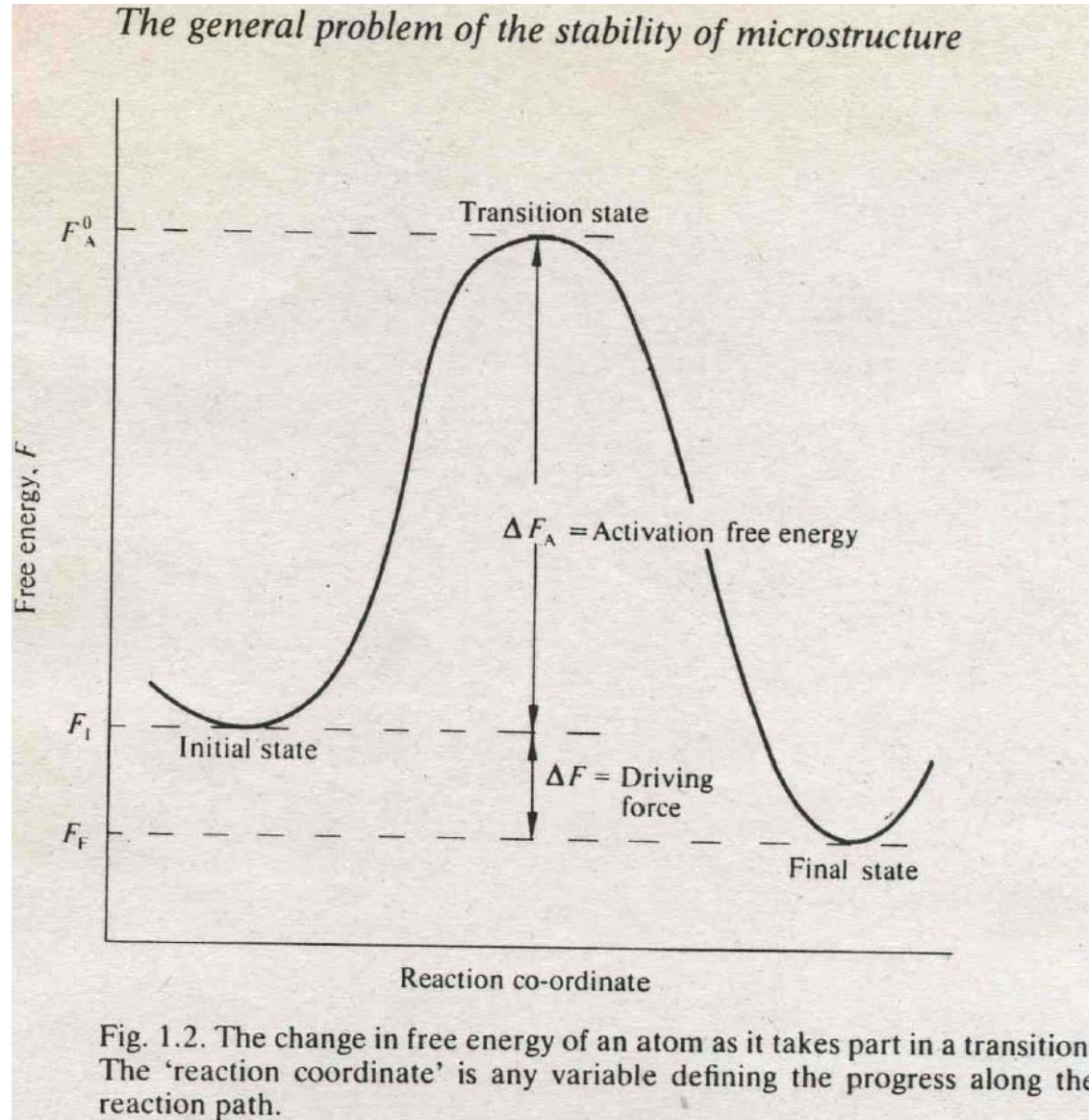


Figure 21 Heat capacity versus temperature of CuZn (β -brass) alloy. [After F. C. Nix and W. Shockley, *Revs. Mod. Physics* **10**, 1 (1938).]

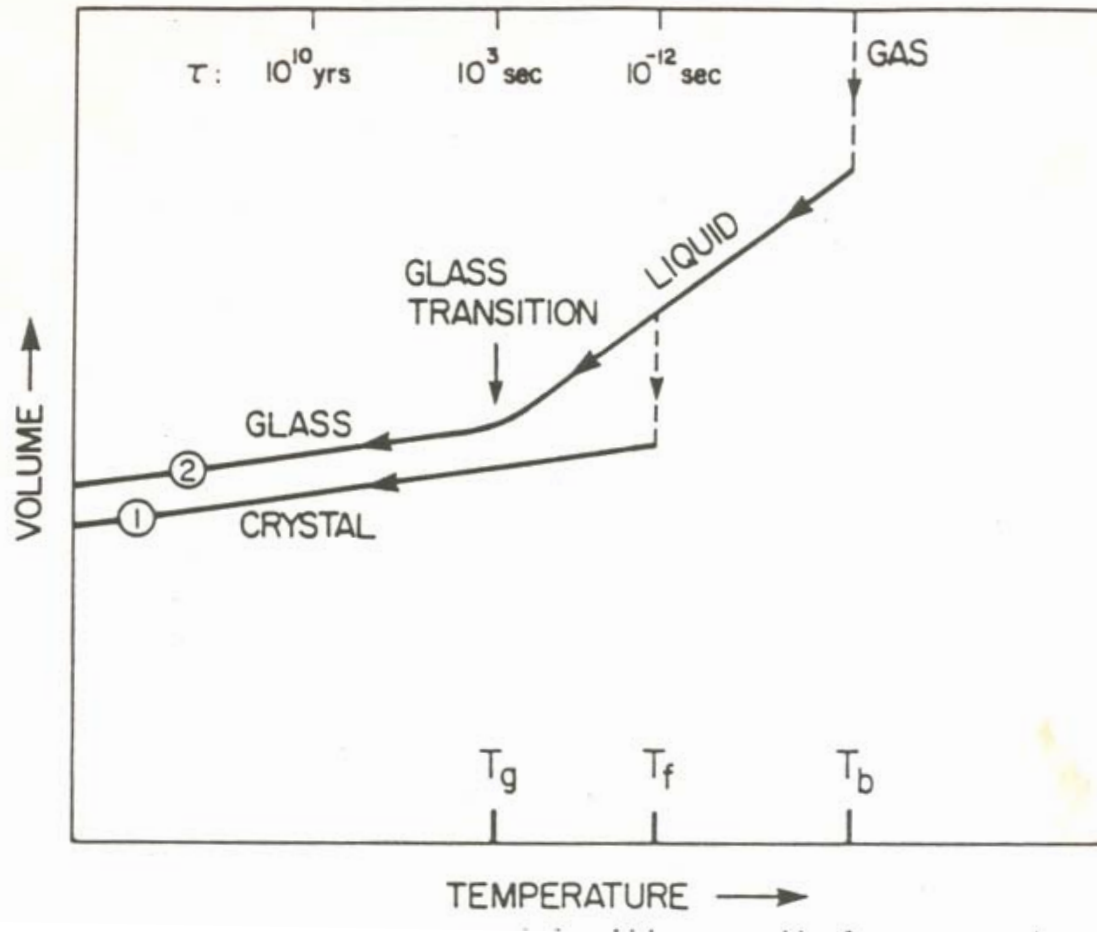
Stability of Nanostructures - Scheme



Stability of Nanostructures – Free Energy



Two General Cooling Paths – Crystalline vs. Amorphous Phases



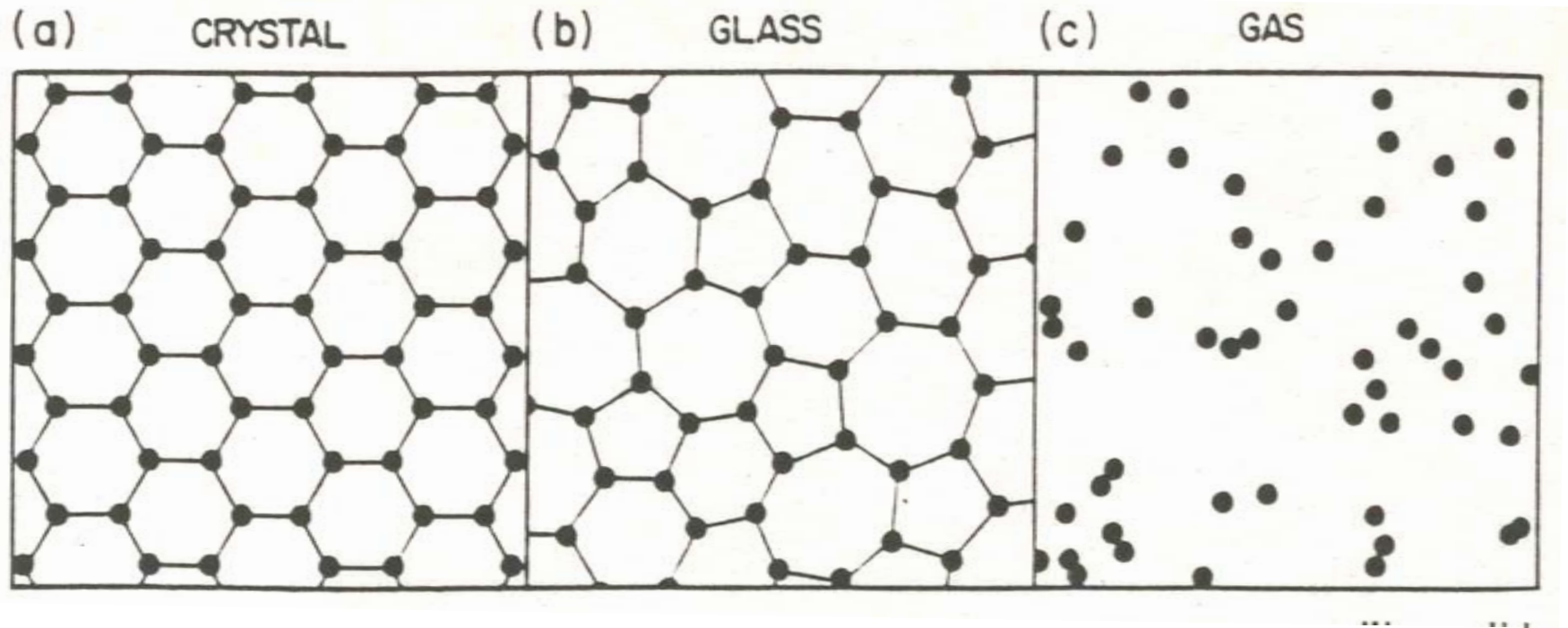
Route ①: path to the crystalline solid state

➔ discontinuous

Route ②: rapid quenching to the amorphous solid

➔ continuous

Schematic Sketches of Atomic Arrangements

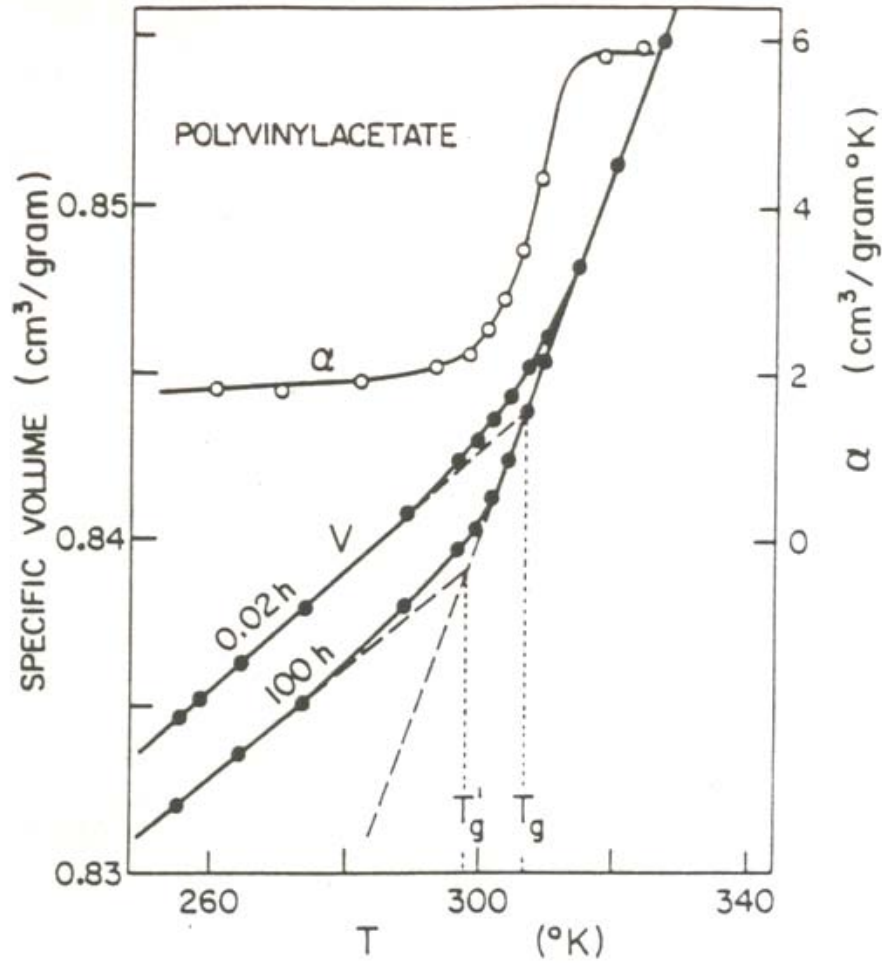


(a) Crystal = The bond lengths and angles are exactly (almost) equal.

(b) Amorphous = High degree of local correlation.

(c) Gas = The particles are rarely correlated.

Glass-Transition Temperature vs. Cooling Rate



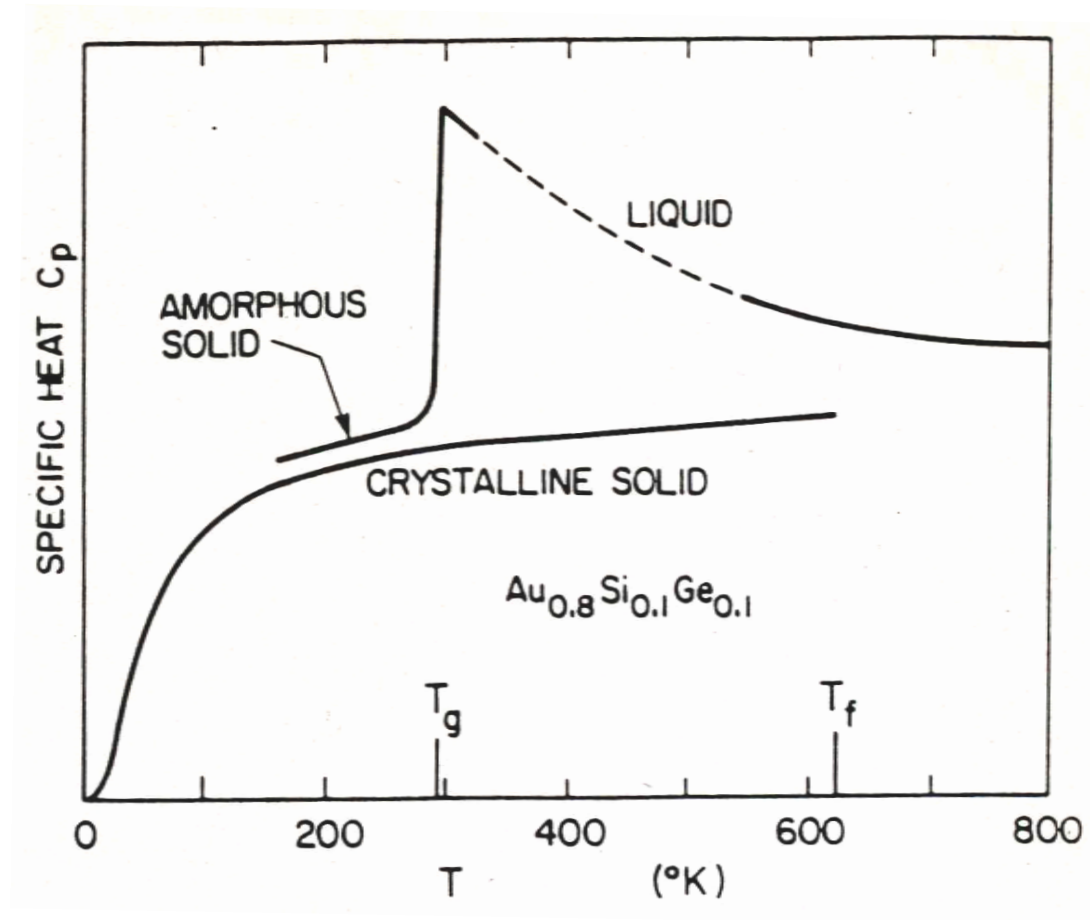
Liquid-glass transition

Relaxation



KAL

Specific Heat of Amorphous Phase



No Latent Heat

Second-Order Transition

Glass - Liquid Transition

Examples of Applications for Amorphous Solids

TABLE 1.2 Some examples of applications of amorphous solids

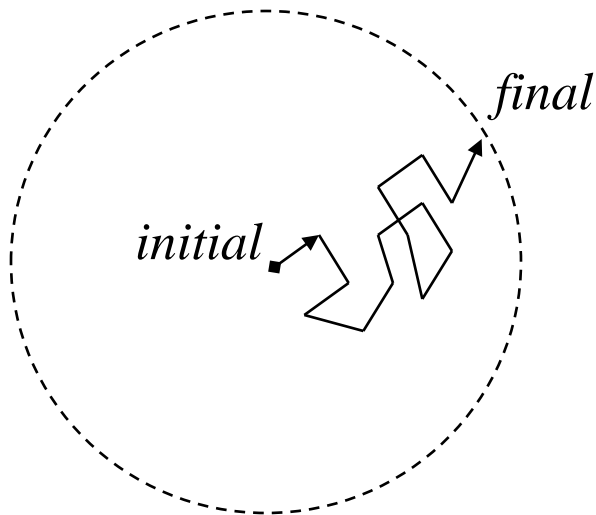
<i>Type of Amorphous Solid</i>	<i>Representative Material</i>	<i>Application</i>	<i>Special Properties Used</i>
Oxide glass	$(\text{SiO}_2)_{0.8}(\text{Na}_2\text{O})_{0.2}$	Window glass, etc.	Transparency, solidity, formability as large sheets
Oxide glass	$(\text{SiO}_2)_{0.9}(\text{GeO}_2)_{0.1}$	Fiber optic waveguides for communications networks	Ultratransparency, purity, formability as uniform fibers
Organic polymer	Polystyrene	Structural materials, “plastics”	Strength, light weight, ease of processing
Chalcogenide glass	Se, As_2Se_3	Xerography	Photoconductivity, formability as large-area films
Amorphous semiconductor	$\text{Te}_{0.8}\text{Ge}_{0.2}$	Computer-memory elements	Electric-field-induced amorphous \leftrightarrow crystalline transformation
Amorphous semiconductor	$\text{Si}_{0.9}\text{H}_{0.1}$	Solar cells	Photovoltaic optical properties, large-area thin films
Metallic glass	$\text{Fe}_{0.8}\text{B}_{0.2}$	Transformer cores	Ferromagnetism, low loss, formability as long ribbons

Amorphous InGaZnO Semiconductor for Thin-Film Transistor (TFT)

Diffusion

- Redistribution of atoms from regions of high concentration of mobile species to regions of low concentration.
- It occurs at all temperatures.
- The diffusivity has an exponential dependence on T .

Random Walk



Age of Universe $\sim 10^{17}$ sec (10^{10} years)

Gas : $D \sim 1 \text{ cm}^2/\text{s}$ \longrightarrow $(Dt)^{1/2} \sim 3000 \text{ km}$

Liquid : $D \sim 10^{-5} \text{ cm}^2/\text{s}$ \longrightarrow $(Dt)^{1/2} \sim 10 \text{ km}$

Solid : $D \sim 10^{-8} \text{ cm}^2/\text{s}$ \longrightarrow $(Dt)^{1/2} \sim 300 \text{ m}$

Fick's Law

Fick's 1st Law

$$\vec{J} = -D \frac{\partial C}{\partial x}$$

\vec{J} : diffusive flux (atoms/cm²•sec)

D : diffusion coefficient (cm²/sec)

C : atomic concentration (atoms/cm³)

X : distance (cm)

Fick's 2nd Law

If D is independent of C , then

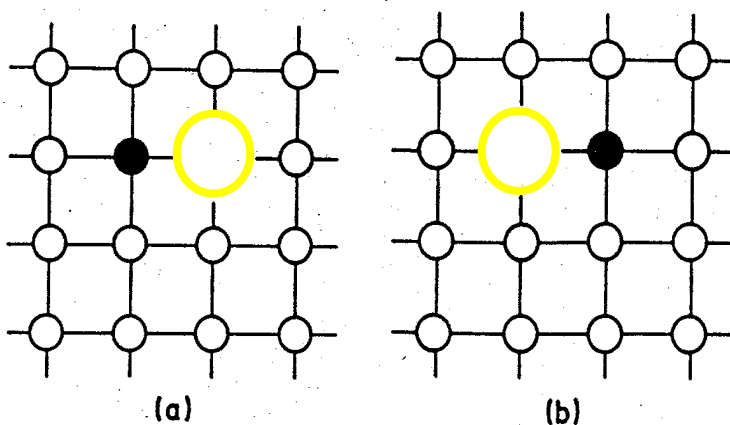
$$\nabla \cdot \vec{J} + \frac{\partial C}{\partial t} = 0$$



$$D \frac{\partial^2 C}{\partial x^2} = \frac{\partial C}{\partial t}$$

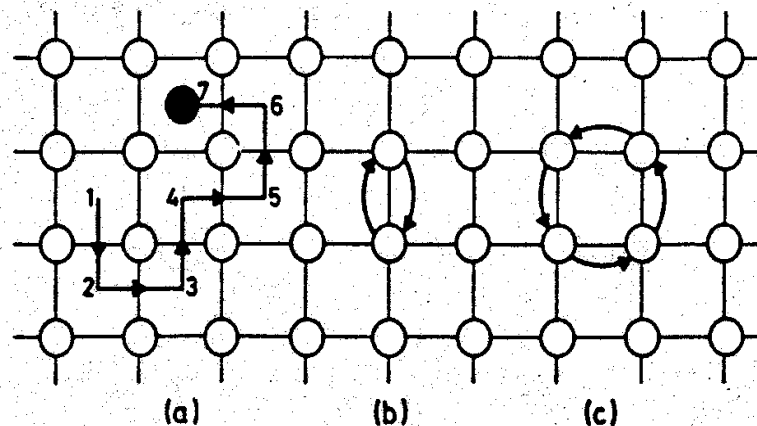
How Do Atoms Diffuse?

<Vacancy Mechanism>



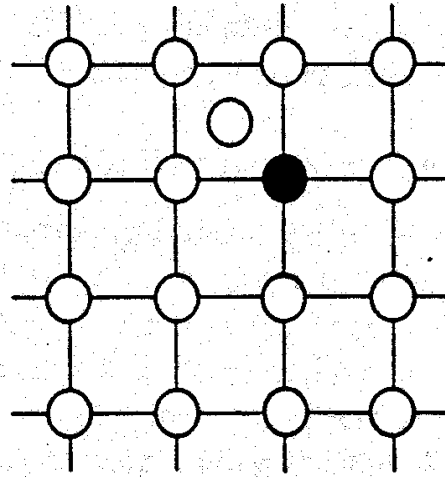
- (a) Before jumping
- (b) After jumping into the right-hand side

<Interstitial Mechanism>



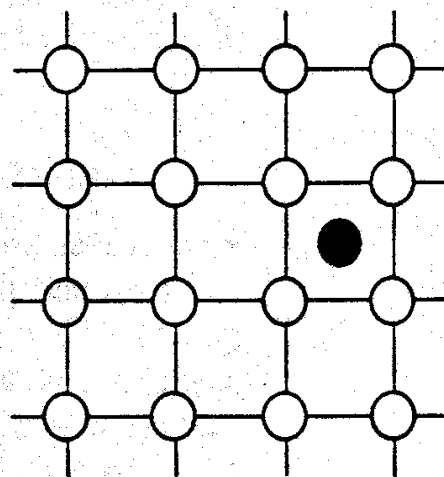
- (a) Direct interstitial mechanism
- (b) Direct exchange of a pair of atoms
- (c) Ring mechanism

Kick-Out Mechanisms



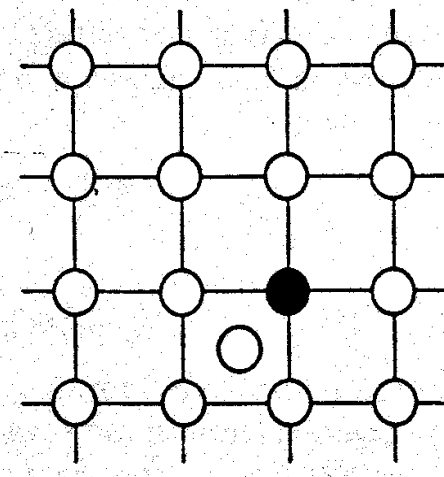
(a)

(a) Interstitial Si has approached substitutional Au.



(b)

(b) Au has exchanged its original position with Si.

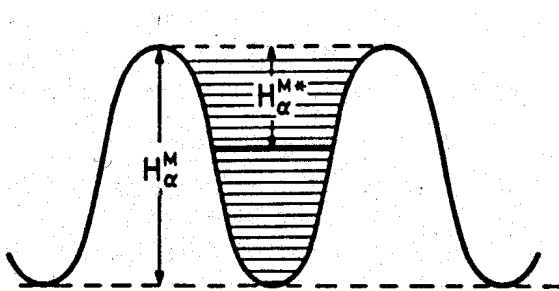


(c)

(c) Au has re-occupied a regular site by kicking a Si atom into an interstice.

ex) Au diffusion in *c*-Si

How Fast? – Thermal Activation



Thermally assisted energy-release mechanism via the vibrational state marked by the heavy horizontal line.

For interstitial diffusion

$$D = D_0 \exp\left(-\frac{\Delta H_m}{k_B T}\right)$$

Activation enthalpy : $Q = \Delta H_m \sim 1 \text{ eV}$

Prefactor: $D_0 \sim 10^{-2} - 10^{-3} \text{ cm}^2/\text{sec}$

For substitutional diffusion

$$D = D_0 \exp\left(-\frac{\Delta H_f + \Delta H_m}{k_B T}\right)$$

Activation enthalpy : $Q = \Delta H_f + \Delta H_m \sim 3 - 5 \text{ eV}$

Prefactor: $D_0 \sim 10 - 10^{-1} \text{ cm}^2/\text{sec}$

Several Points for Self Diffusion

(1) Rough correlation between Q ($= \Delta H_f + \Delta H_m$) and T_m

Interatomic bond strength (cohesive energy) $\uparrow \longrightarrow Q \uparrow T_m \uparrow D \downarrow$

$$Q \sim 20 k_B T_m$$

$$k_B = 8.617 \times 10^{-5} \text{ eV/K}$$

(2) Temperature Dependence

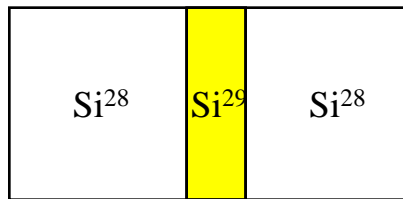
For Ge self-diffusion

$$D = 4.4 \text{ cm}^2/\text{s} \times \exp(-3.4 \text{ eV}/k_B T)$$

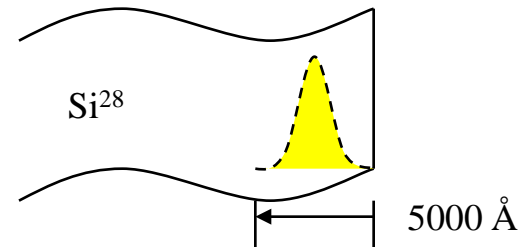
$$\begin{aligned} T_m &= 1211 \text{ K} & D &= 3.1 \cdot 10^2 \text{ \AA}^2/\text{s} & (Dt)^{1/2} &\sim 1000 \text{ \AA} \\ T_m &= 298 \text{ K} & D &= 1.4 \cdot 10^{-41} \text{ \AA}^2/\text{s} & (Dt)^{1/2} &\sim 10^{-19} \text{ \AA} \\ & & & & \text{For } t &= 1 \text{ hour} \end{aligned}$$

(3) Measurements (S.I.M.S.)

By deposition ($\sim 200 \text{ \AA}$)



Implant $\text{Si}^{29} \sim 100 \text{ keV}$



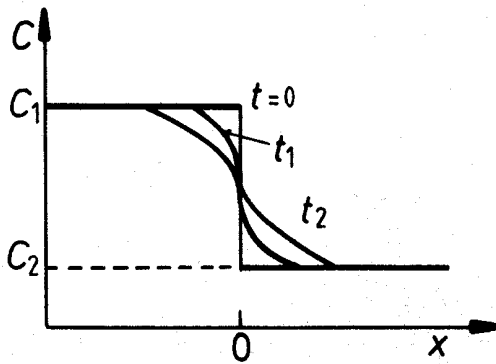
Solution to the Diffusion Equation

Governing Equation

$$D \cdot \nabla^2 C = \frac{\partial C}{\partial t}$$

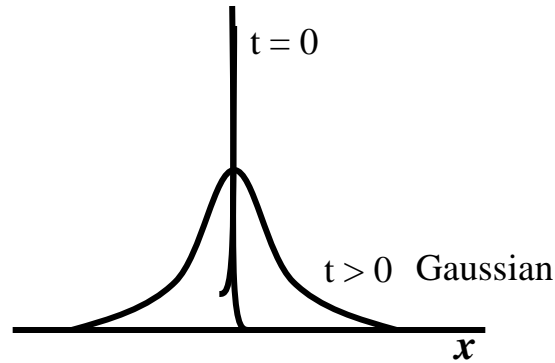
$D > 0$

D independent of C

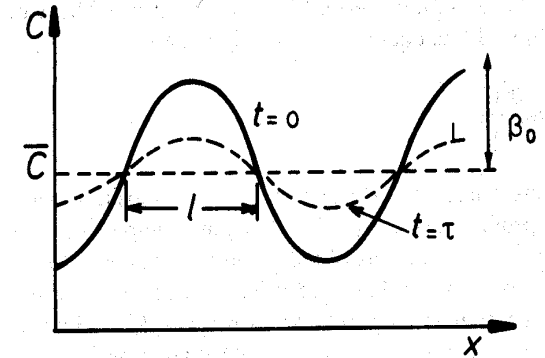


$$C(x) = \frac{C_1 + C_2}{2} - \text{erf}\left(\frac{x}{2\sqrt{Dt}}\right)$$

$$\text{erf}(z) = \frac{2}{\sqrt{\pi}} \int_0^z \exp(-y^2) dy$$



$$C(x) = \frac{\text{Area}}{2\sqrt{\pi Dt}} \exp\left(-\frac{x^2}{4Dt}\right)$$

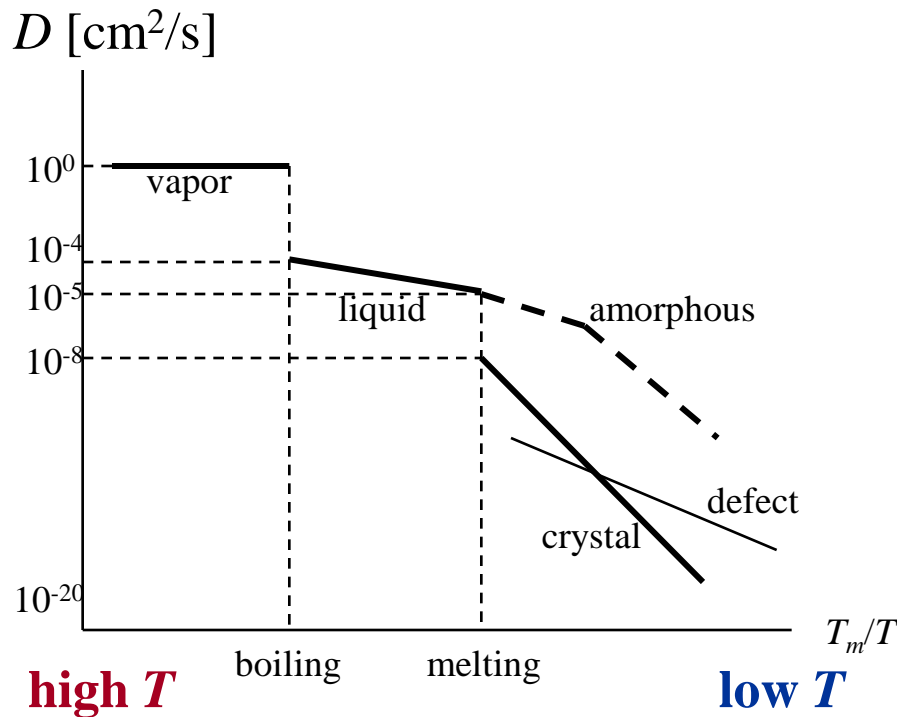


$$C(x) = \bar{C} + \beta_0 \sin\left(\frac{\pi x}{l}\right) \exp\left(-\frac{t}{\tau}\right)$$

$$\tau = \frac{l^2}{\pi^2 D}$$

Superlattice (Si/SiGe)

Empirical Survey of Self Diffusion



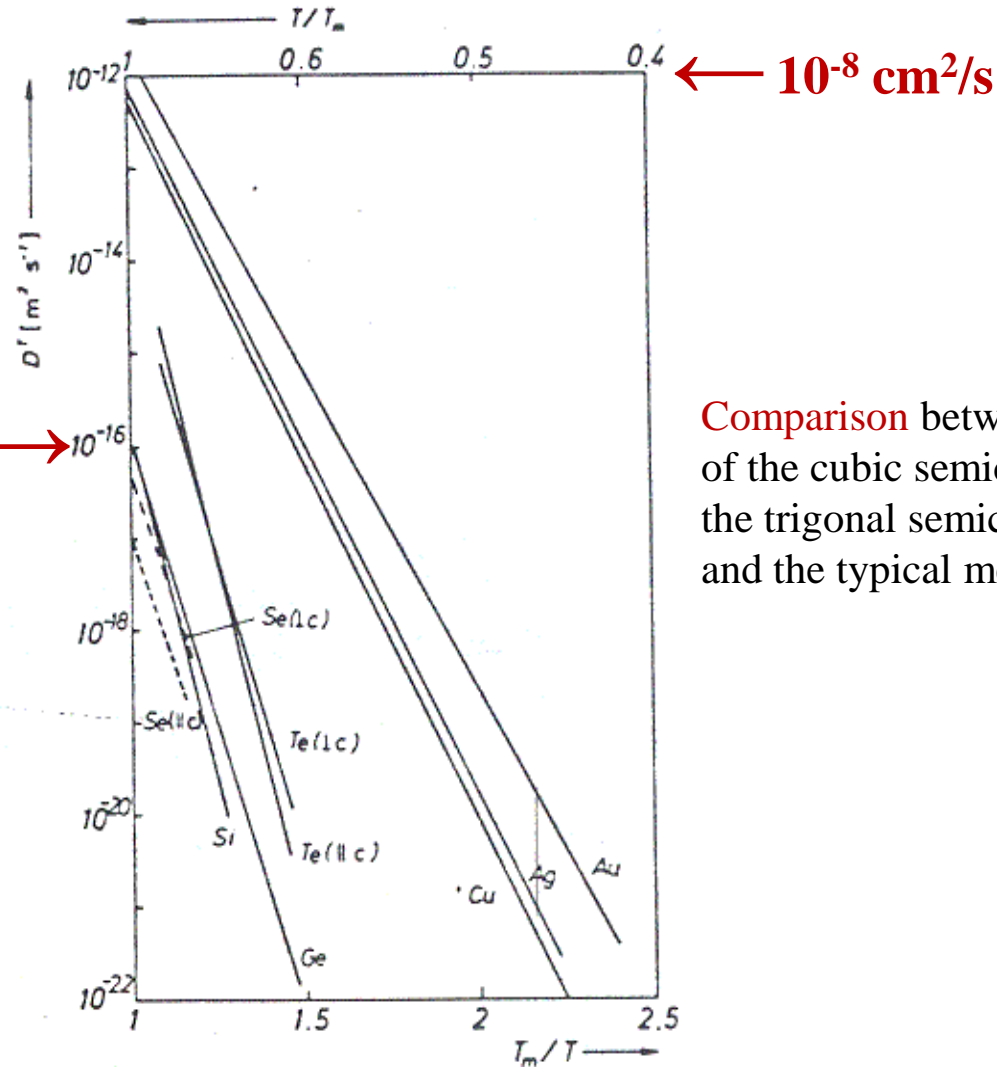
* Extended Structural Defects

- Dislocation
- Grain boundary
- Short circuit: easy diffusion path dominant at low T

* Structure

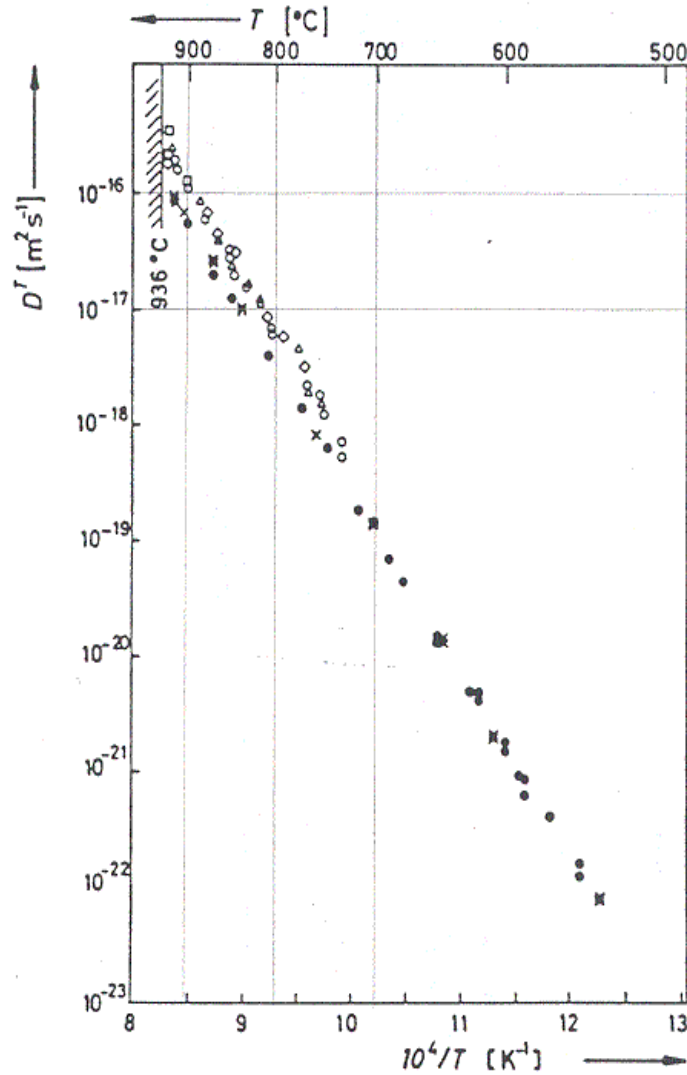
- fcc: $D(T_m) \sim 10^{-8} \text{ cm}^2/\text{s}$
- bcc: $D(T_m) \sim 10^{-7} \text{ cm}^2/\text{s}$
- diamond: $D(T_m) \sim 10^{-12} \text{ cm}^2/\text{s}$

Self Diffusivity



Comparison between the self-diffusivities of the cubic semiconductors Ge and Si, the trigonal semiconductors Te and Se, and the typical metals Cu, Ag, and Au.

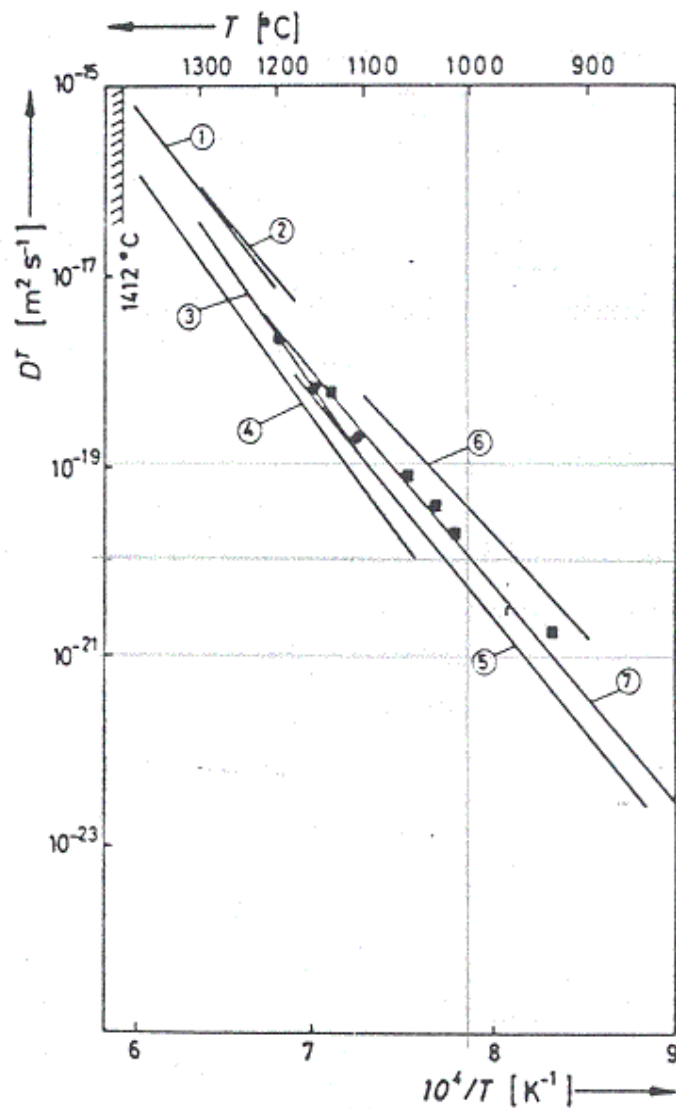
Self Diffusion in Ge



← $10^{-12} \text{ cm}^2/\text{s}$

Tracer self-diffusion coefficient of Ge as a function of temperature. Data are from various groups.

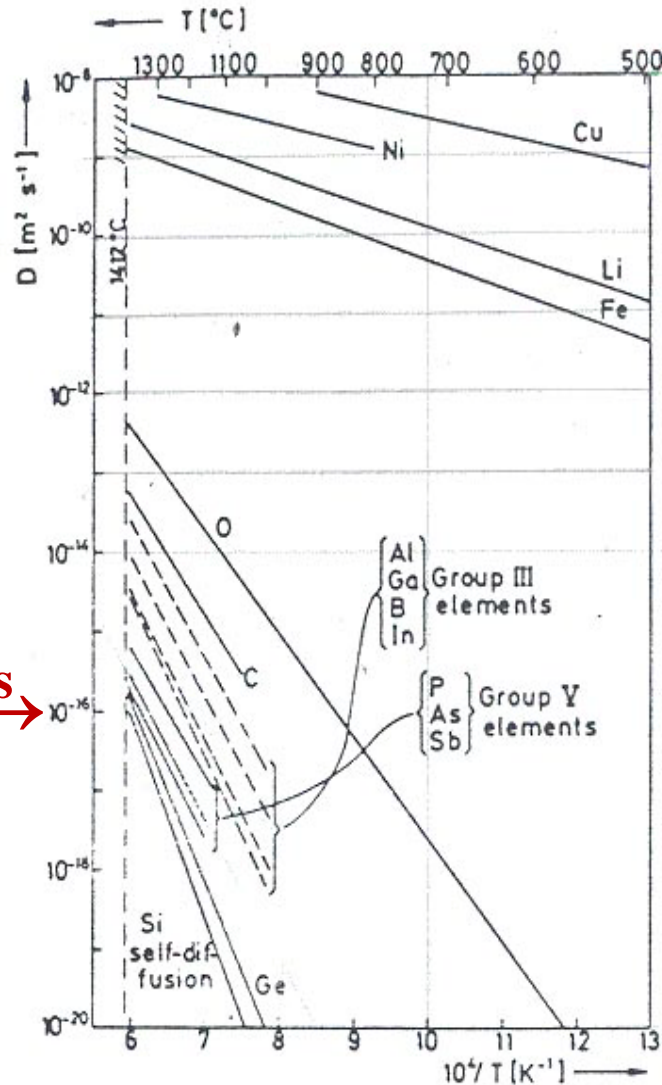
Self Diffusion in Si



← $10^{-12} \text{ cm}^2/\text{s}$

Tracer self-diffusion coefficient of Si as a function of temperature from various groups. Deviations may arise from several reasons which need to be further investigated.

Tracer Diffusivities of Foreign Atoms in Si



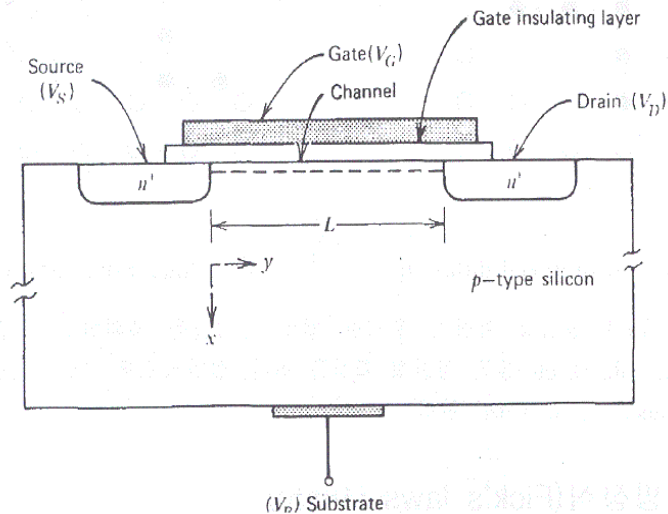
← $10^{-4} \text{ cm}^2/\text{s}$

Survey of the diffusivities of foreign atoms in silicon. Foreign atoms include Cu, Ni, Li, Fe, O, C; group III (Al, Ga, As); group V (P, As, Sb); and Ge. For comparison, Si self-diffusion data are included.

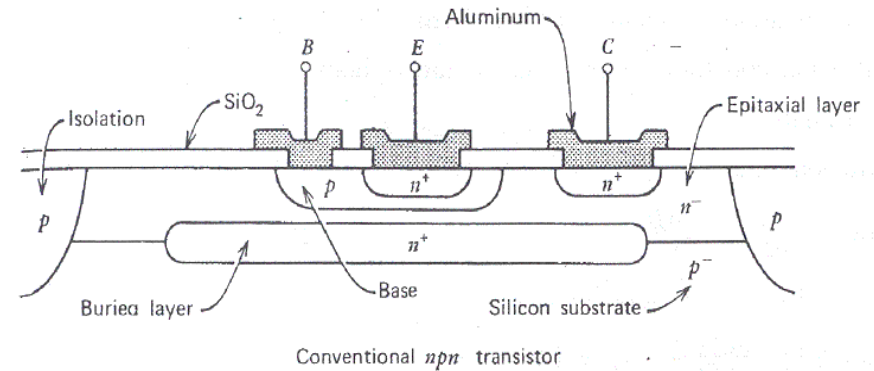
$10^{-12} \text{ cm}^2/\text{s}$ →

Device Applications

- In semiconductor devices, solute atoms control electrical conductivity and n -type (or p -type) doping.
- Concentration and distribution of dopants play a critical role in the device operation.



MOSFET (Metal Oxide Semiconductor Field Effect Transistor)



BJT (Bipolar Junction Transistor)

DIFFUSION ON SEMICONDUCTOR SURFACES

Semiconductor devices continue to get ever smaller, which means that individual defects play an increasingly important role in their performance. In the process of fabricating more innovative, better performing devices, crystal growers have developed an amazing intuition about how atoms and molecules behave on crystal surfaces. Their intuition, formed from knowledge of fundamental atomic-scale processes and honed through experience, concerns such questions as where atoms and molecules stick, how they interact with each other and the substrate, and how they diffuse.

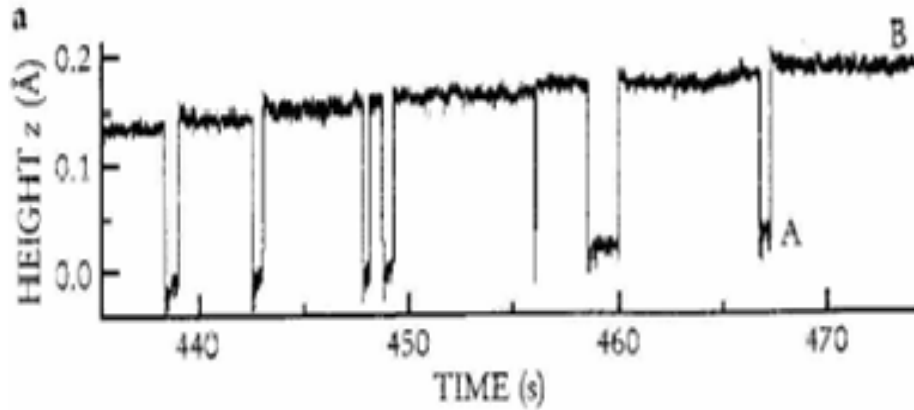
Atomic-resolution imaging techniques show that a good deal of surface physics can be understood with elementary statistical mechanics, but some surprisingly complex behaviors occur even in simple systems.

Harold J. W. Zandvliet, Bene Poelsema,
and Brian S. Swartzentruber

rapidly and quickly finds another atom with which to form an adsorbed dimer. Adsorbed dimers can be bound either on top of, or between, the substrate dimer rows and can have their dimer bonds oriented parallel or perpendicular to the rows. Dimers on top of the substrate rows can rotate, changing their orientation from parallel to perpendicular and back. They can also diffuse, both along and across substrate rows. The stability of binding sites, along with rotational and diffusion barriers, can all be readily extracted from real-time scanning tunneling microscopy (STM) experiments—with the help of elemen-

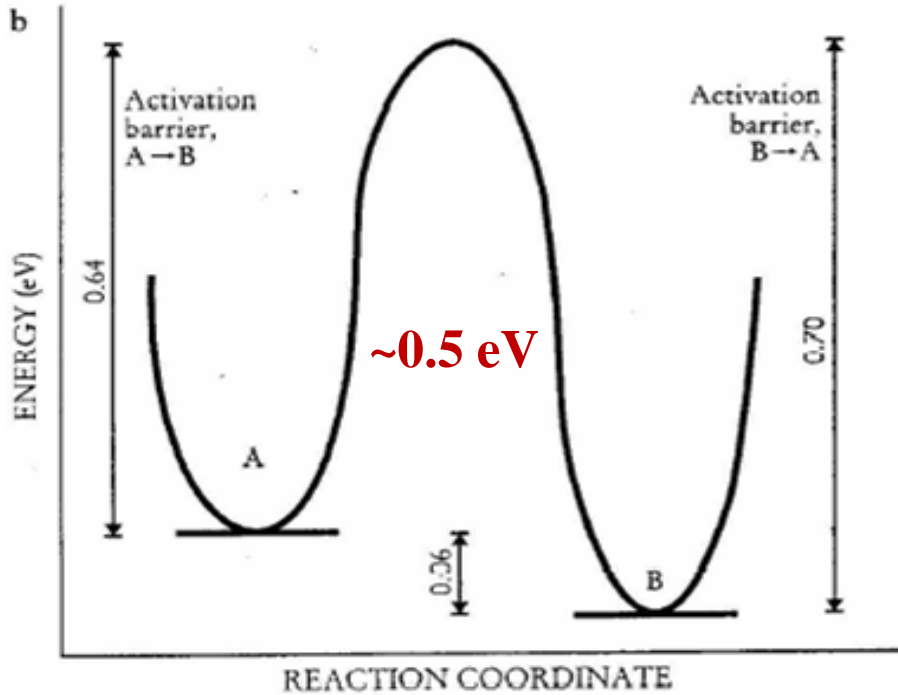
Physics Today (July 2001)

Individual Si Atom and Dimer on Si (001)

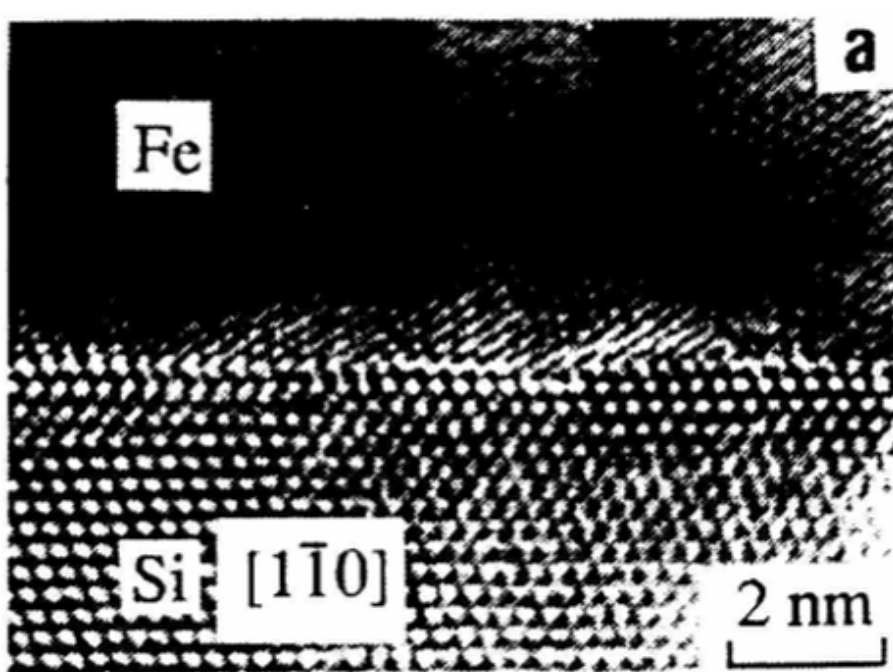


Height z as function of time
(Scanning tunneling microscope tip)

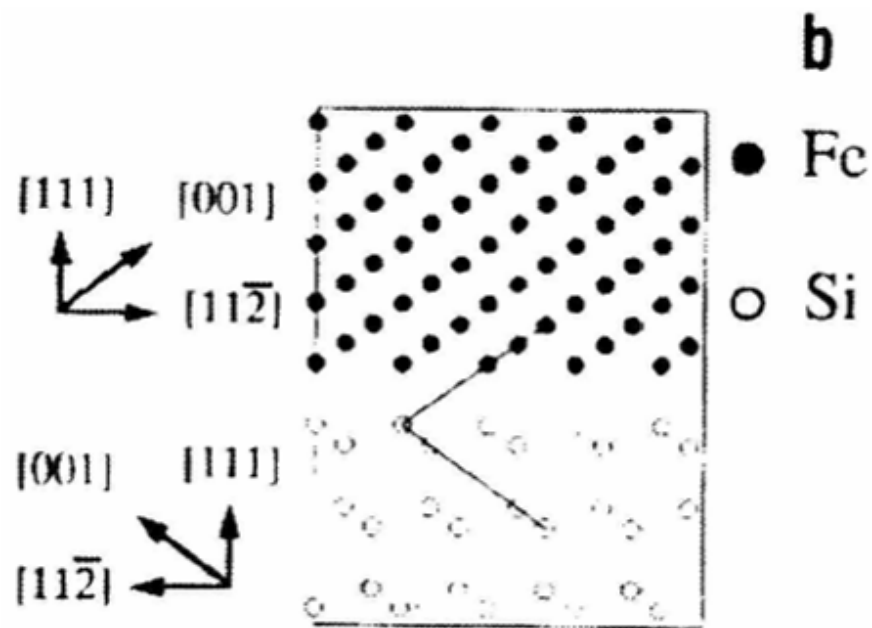
- Transition between A and B
- Different transition rates



Energy vs. coordinate



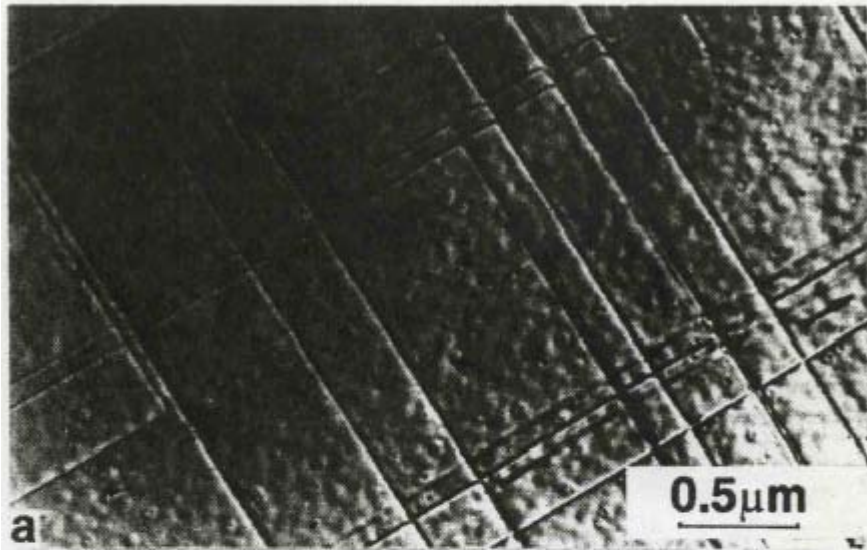
Atomic image of α -Fe/Si interface along $[110]$ Si direction.



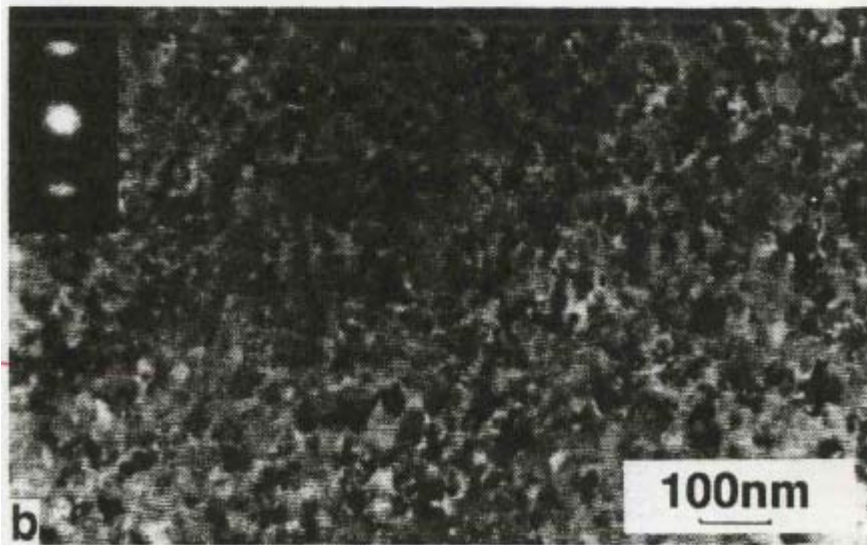
A schematic diagram showing the twinned epitaxy.

Appl. Phys. Lett.

Plan-View TEM: $Si_{1-x}Ge_x$ Epitaxy on Si (001)

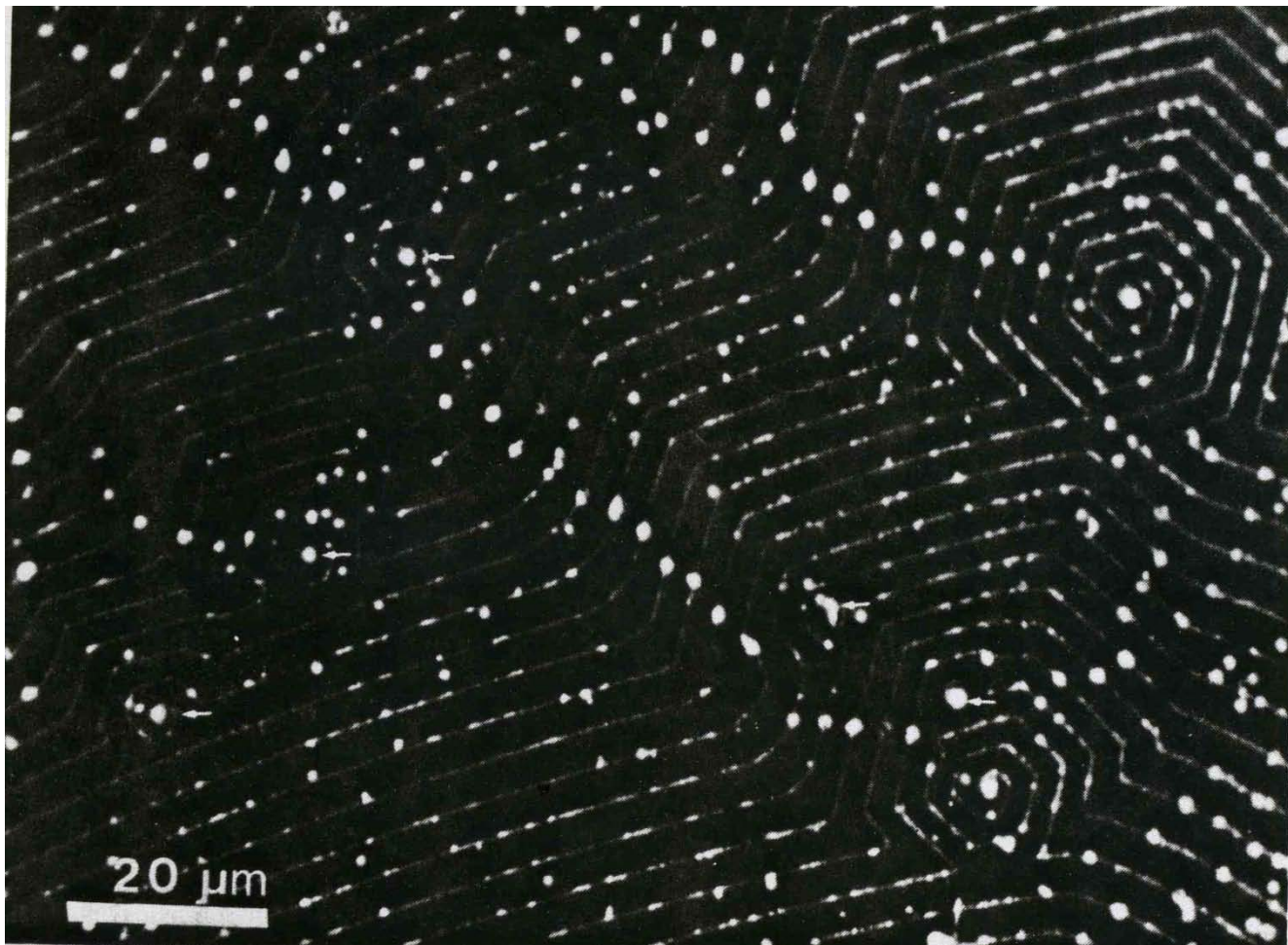


The average dislocation distance
- measured directly.

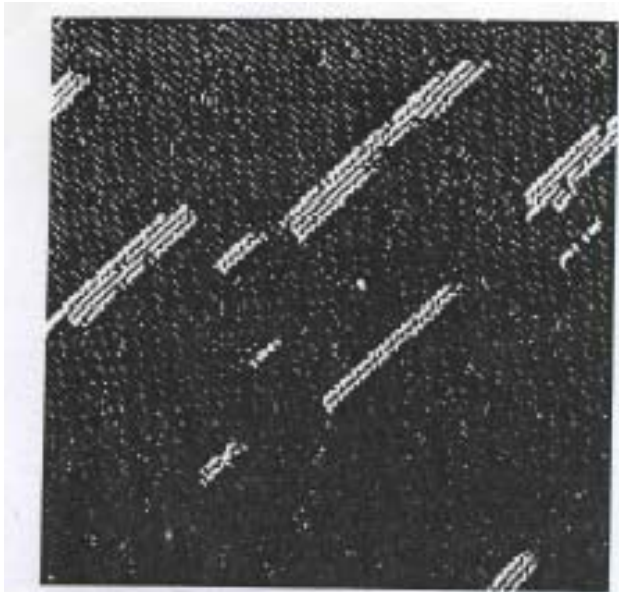


Distance of Moire' fringes

Spiral Growth from Screw Dislocations in SiC

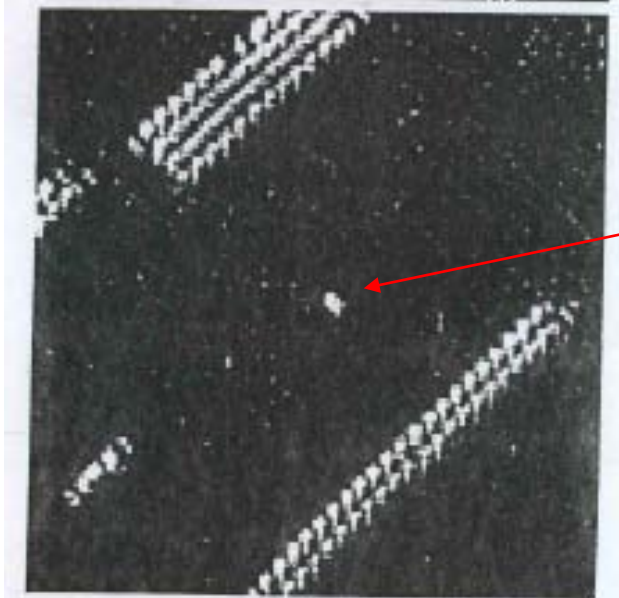


STM: Nanostructural Growth of Si on Si (001)



Islands – anisotropic
Measured by STM

60 nm × 60 nm



Single dimer

25 nm × 25 nm

Growth Characteristics – Silicon (001) Surface

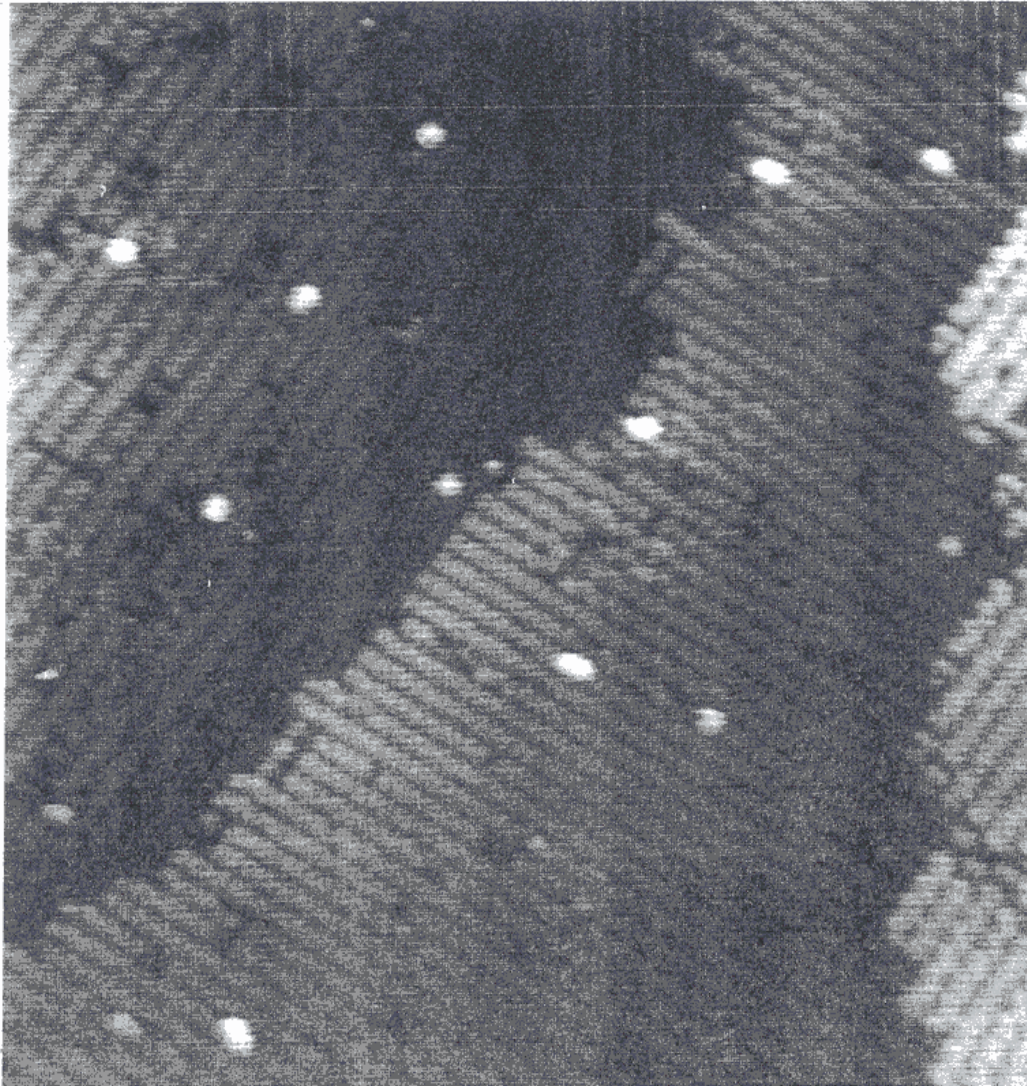


FIGURE 1. A SCANNING tunneling microscope image of a silicon (001) surface after the deposition of a small amount of Si at room temperature. The image shows two single-layer steps (the jagged interfaces) separating three terraces. Because of the tetrahedral bonding configuration in the silicon lattice, dimer row directions are orthogonal on terraces joined by a single-layer step. The area pictured is 30×30 nm.

Bandgap Engineering – Si/Ge Superlattice

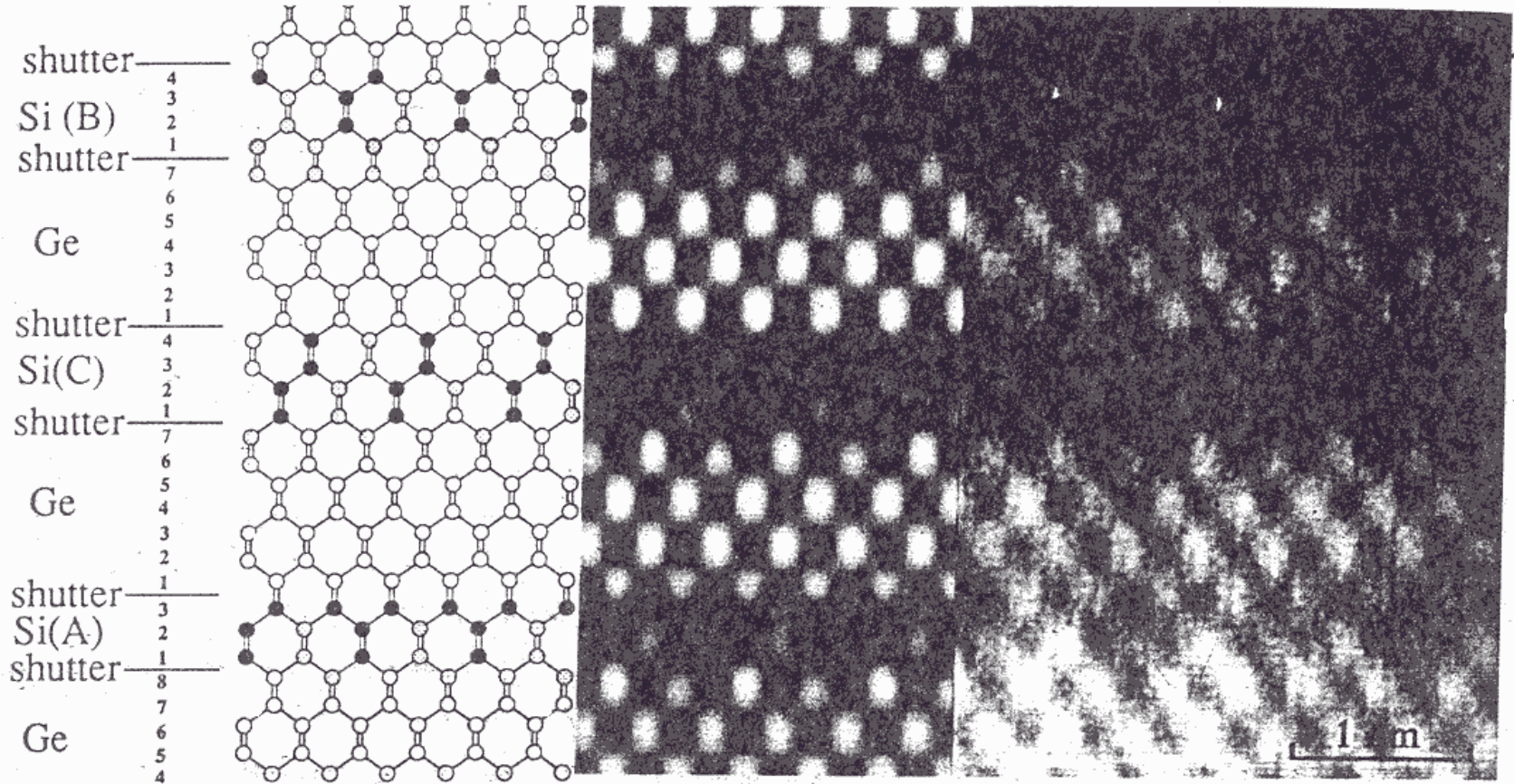
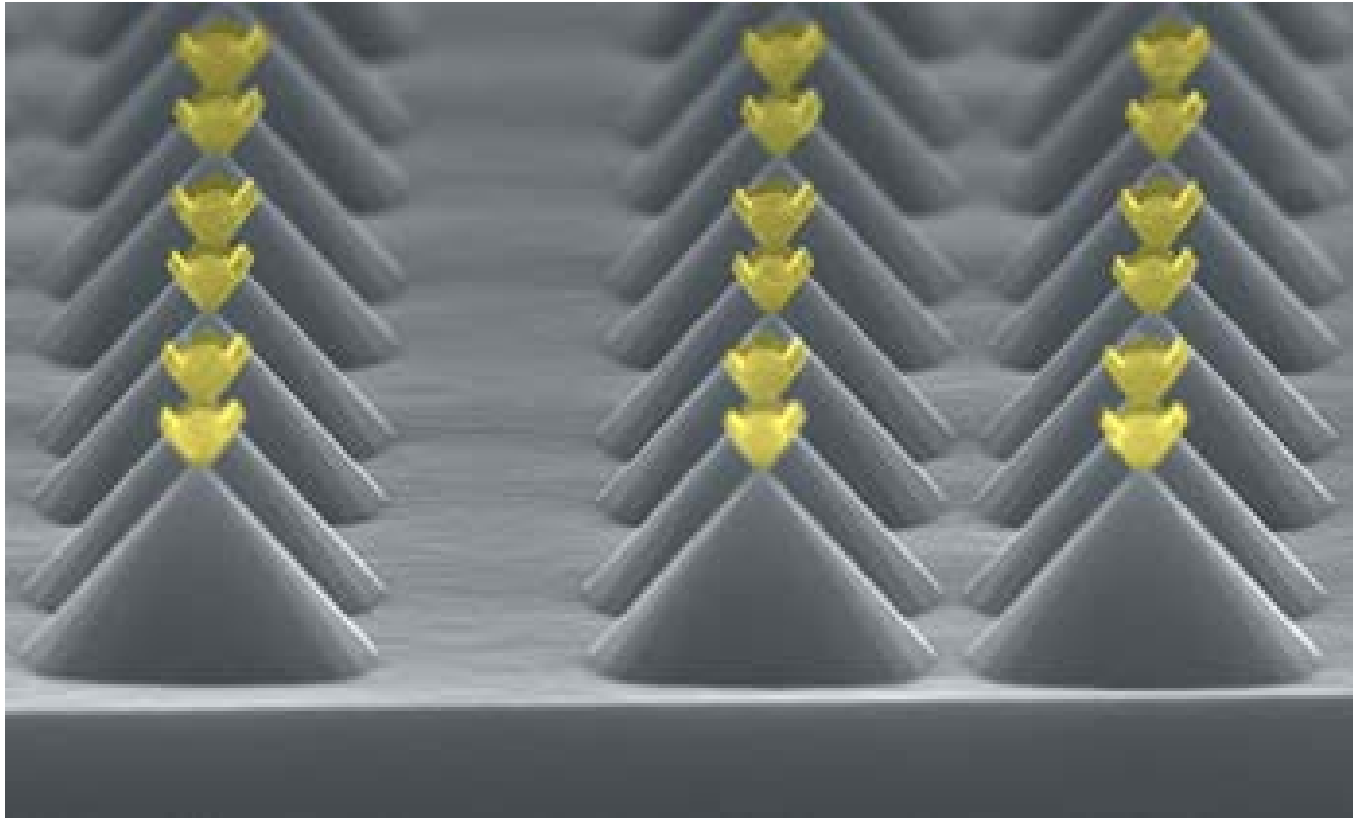


FIG. 4. A [110]-Z-contrast electron microscope image of a nominal $(\text{Si}_4\text{Ge}_8)_{24}$ superlattice revealing unexpectedly complex interfacial arrangements that developed during growth. The schematic and simulation show the structures expected to arise through a Si/Ge atomic exchange process at growing step edge [D. E. Jesson, S. J. Pennycook, and J.-M. Baribeau, *Phys. Rev. Lett.*, **66**, 750 (1991)]. Open circles represent Ge columns, solid circles Si columns, and shaded circles alloy columns.

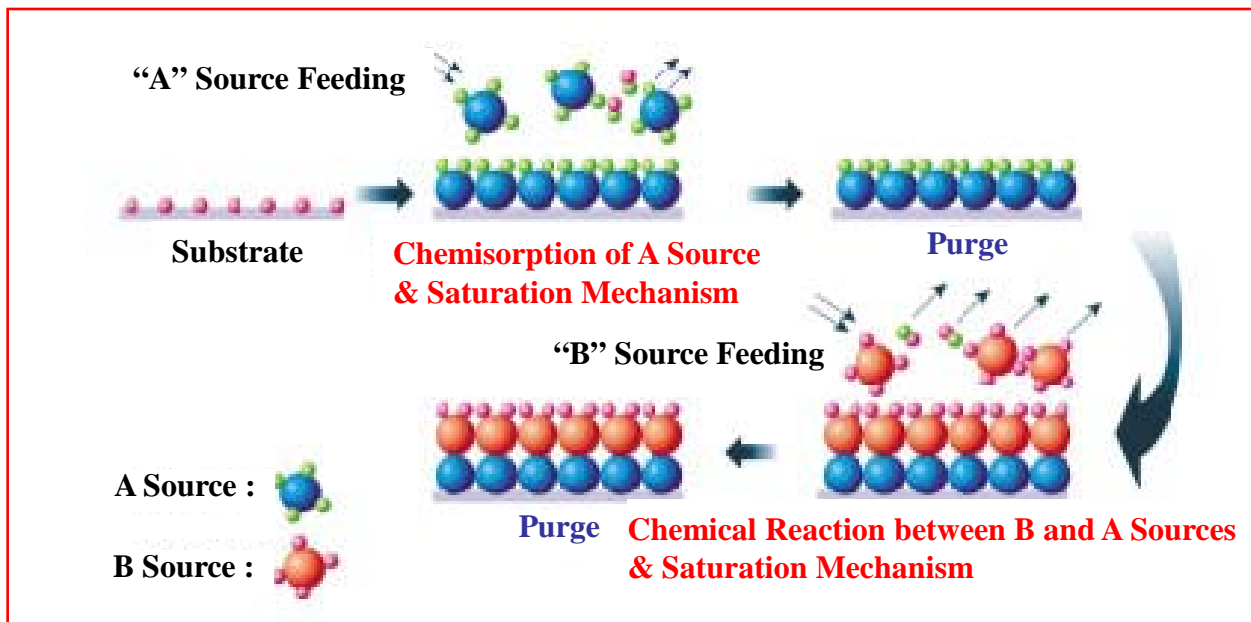
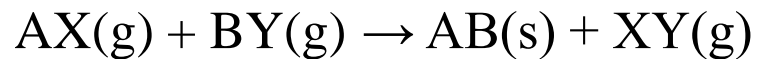
Gold Nanopyramids on Silicon Pedestals



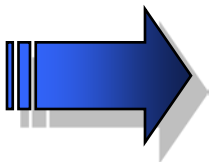
Joel Henzie and Teri W. Odom, Northwestern University, J. Phys. Chem. B (2006)

The orientation-dependent optical properties of the nanoparticle arrays have revealed new insight into the interaction between light and materials at the nanoscale. These structures are also being explored in applications such as chemical /biological sensing and nanophotonics.

Atomic Layer Deposition (ALD)



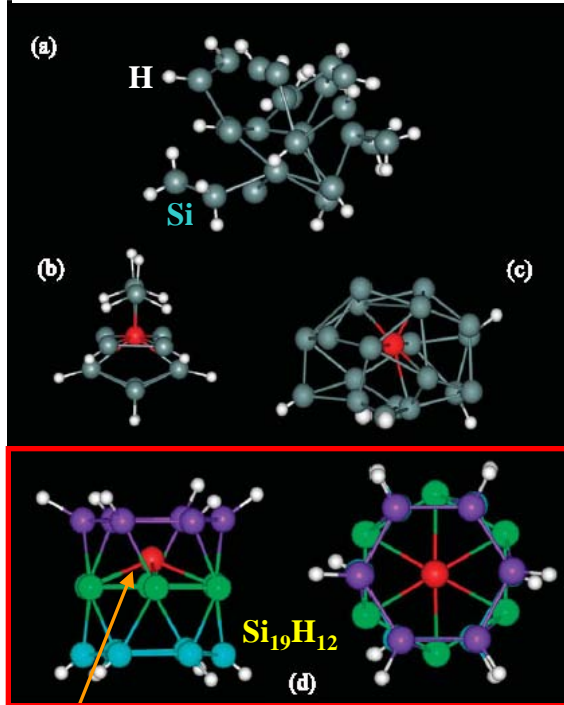
Advantages of ALD



- Accurate and simple thickness control.
- Good reproducibility.
- Sharp interfaces.
- Low processing temperature.
- Uniform, conformal, and dense films.

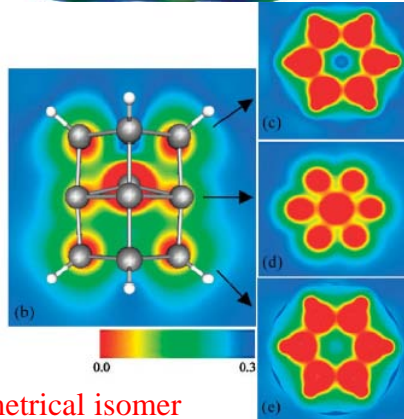
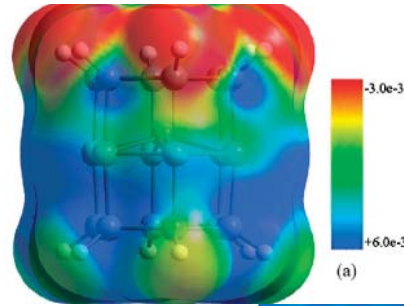
Controlled Growth of Silicon Nanocrystals in a Plasma Reactor

Hydrogenated Si nanoparticles in SiH₄ plasma reactor @ 300 K



(Large dipole moment
→ “off center” of internal Si)

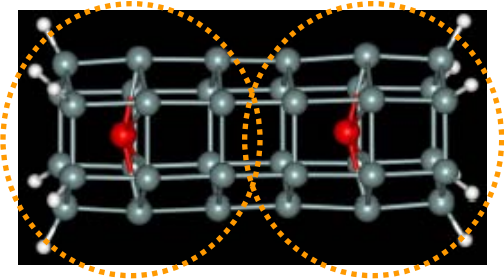
Electron density of Si₁₉H₁₂ isomer with cylindrical configuration



Geometrical isomer
(30° rotation of center hexagon ring)

Phys. Rev. Lett. **95**, 165502 (2005)

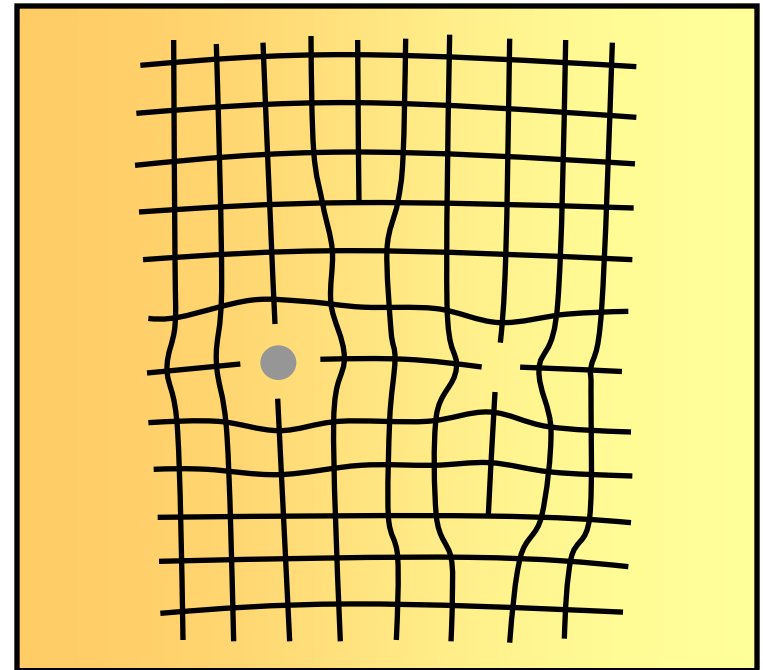
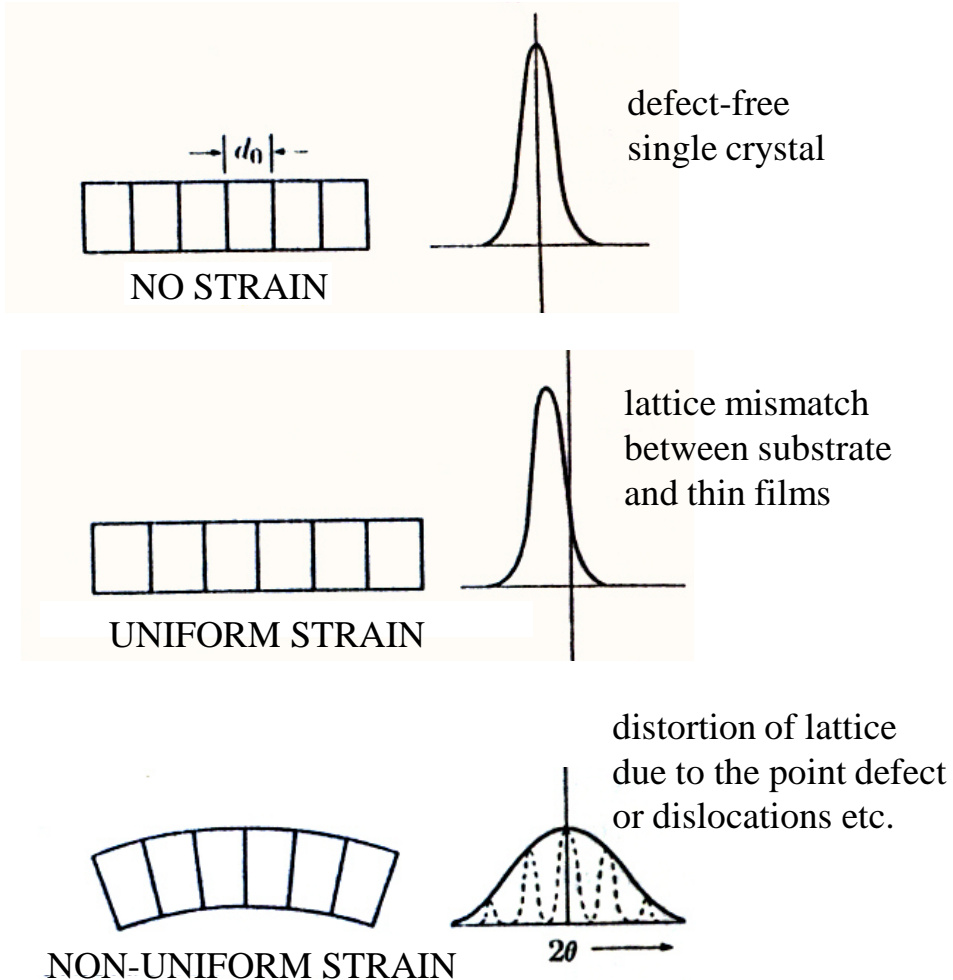
Strong permanent dipole moment (1.9 D)
→ 2 building blocks align themselves
→ Beginning of nanowire formation



Molecular Dynamic (MD) Simulations 이용: CVD Plasma -- Si Nanostructures의 Growth Mechanisms

Amorphous, H-Rich Crystalline, Poor Crystalline, or Tubelike Si₁₉H₁₂

Non-Uniform Distribution of Local Strain



Non-Uniform Local Strain

Point Defects, Off-Stoichiometry, Stacking Faults, Dislocations, etc.

A SURFACE VIEW OF ETCHING

Experiments conducted with scanning tunneling microscopes in ultrahigh vacuum reveal a fascinating, step-by-step picture of the etching process.

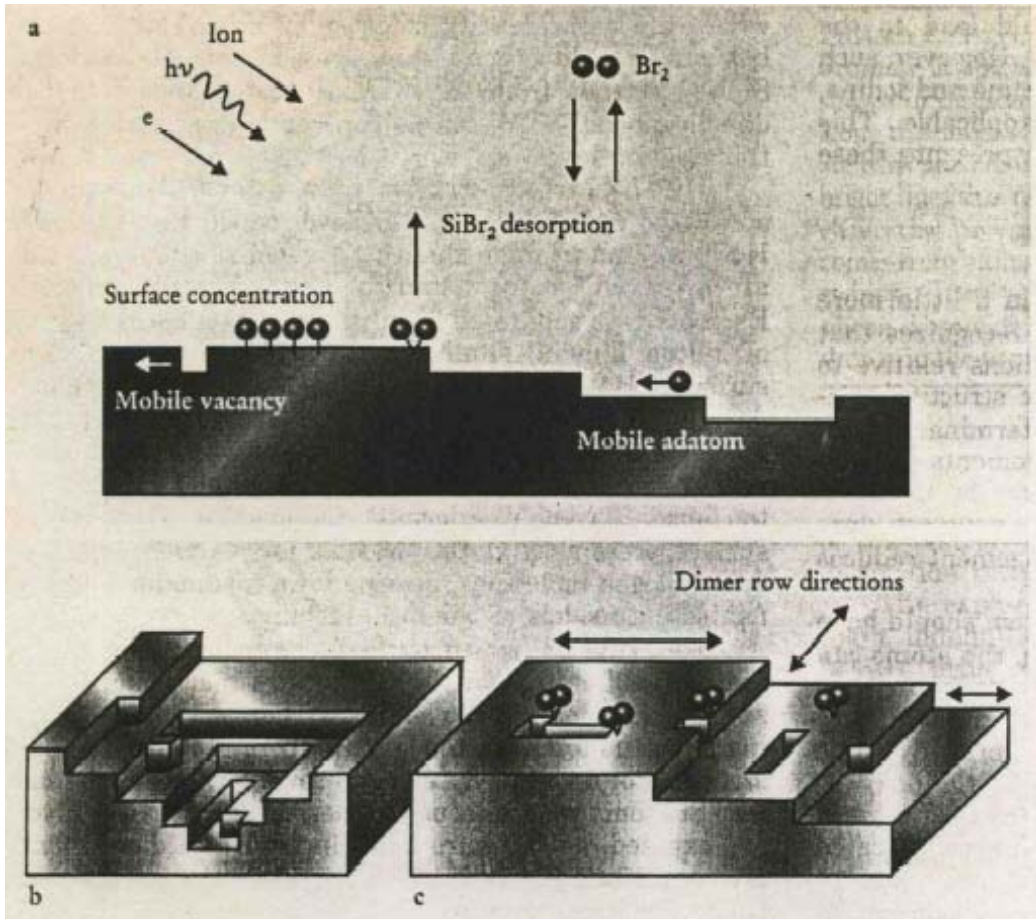
John J. Boland and John H. Weaver

Chemical etching has been practiced since at least the late Middle Ages. In its early form, it involved coating an object, such as a metal plate, with wax, carefully patterning the hardened wax by cutting down through it with a sharpened tool to expose but not penetrate the object's surface and then exposing the object to an etching solution, typically an acid. With time, the etchant molecules in the solution would react with atoms of the exposed surface to form reaction products that would dissolve, thereby removing material from the surface.

exposed to gaseous molecules, rather than to liquids, and the etch products are desorbed into the vapor. Since desorption requires energy to break surface bonds, temperatures as high as 900 K may be needed. In many cases, therefore, it is advantageous to alter the surface chemistry and enhance the formation of volatile species. Numerous so-called assisted etching techniques have been developed to increase etching rates, to achieve directed or anisotropic etching and to make etching possible, at reduced temperatures, for even the most inert materials.

Physics Today (Aug. 1998)

Schematic views of etching - starting with a silicon (100) surface

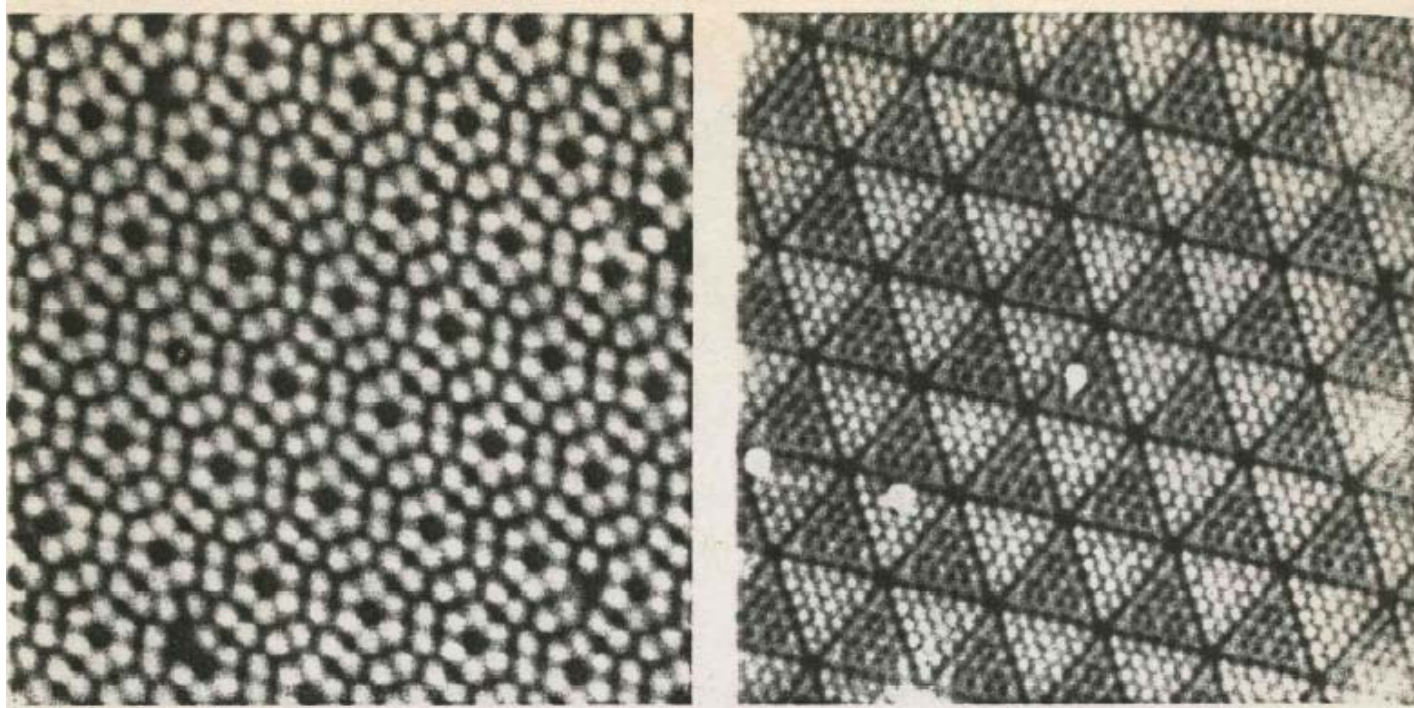


(a) Being exposed primarily to bromine molecules, but also to electrons, protons and ions

(b) Deeply indented surface

(c) Desorption at different surface sites.

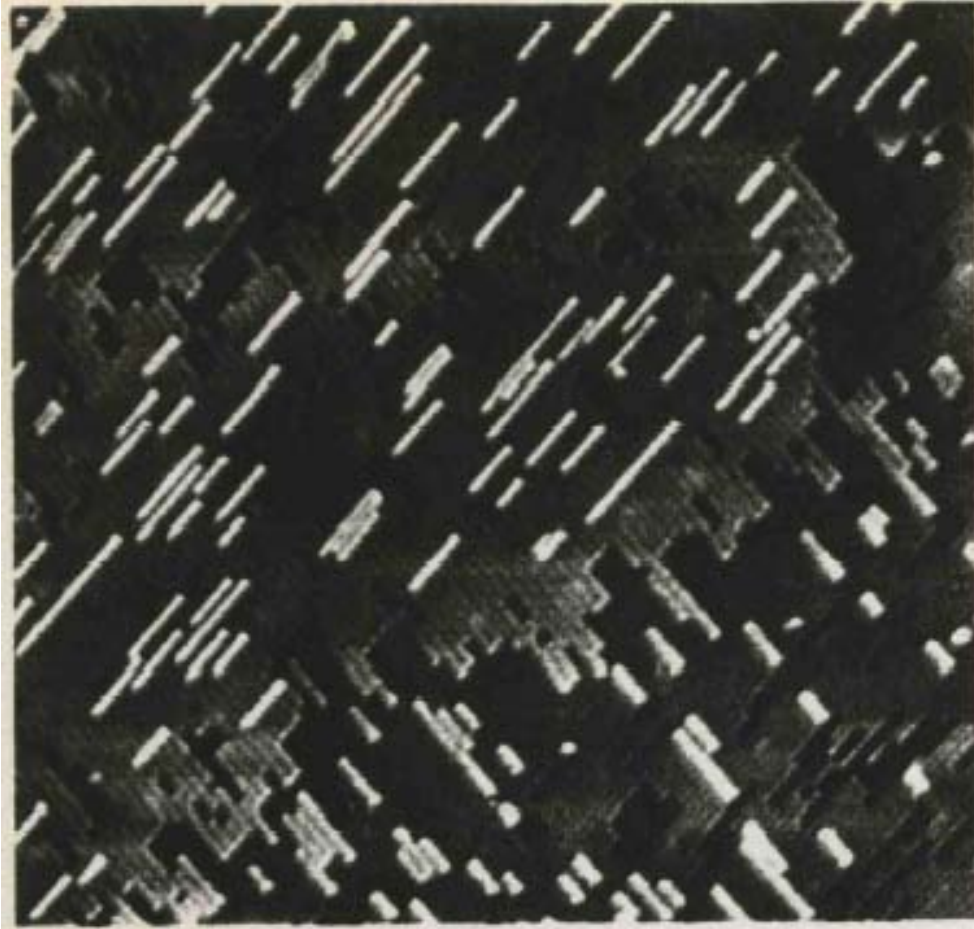
Before and after the removal of adatoms from a reconstructed 7×7 (111) surface as imaged by STM



The adatom layer of the clean Si(111) 7×7 surface.

The rest layer following removal of the adatom layer by bromine etching at 675 K.

Silicon (100): STM Image (55 × 55 nm²)

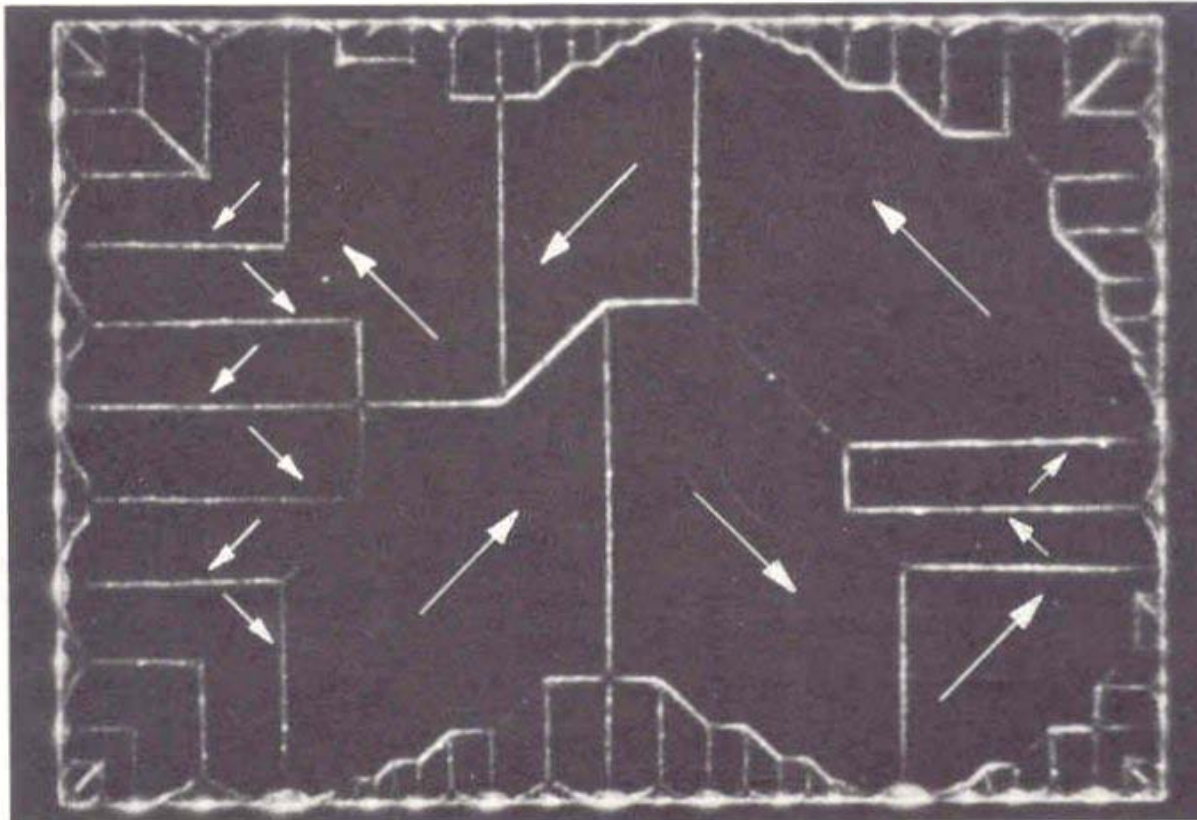


**The dark areas represent pits,
one atom layer deep.**

**The bright lines are silicon
dimer chain.**

Ferromagnetic Domains in a Single Crystal

Single Crystal Ni



C-Ni

Figure 27 Ferromagnetic domain pattern on a single crystal platelet of nickel. The domain boundaries are made visible by the Bitter technique. The direction of magnetization within a domain is determined by observing growth or contraction of the domain in a magnetic field. (After R. W. De Blois.)

Magnetic Domain Width

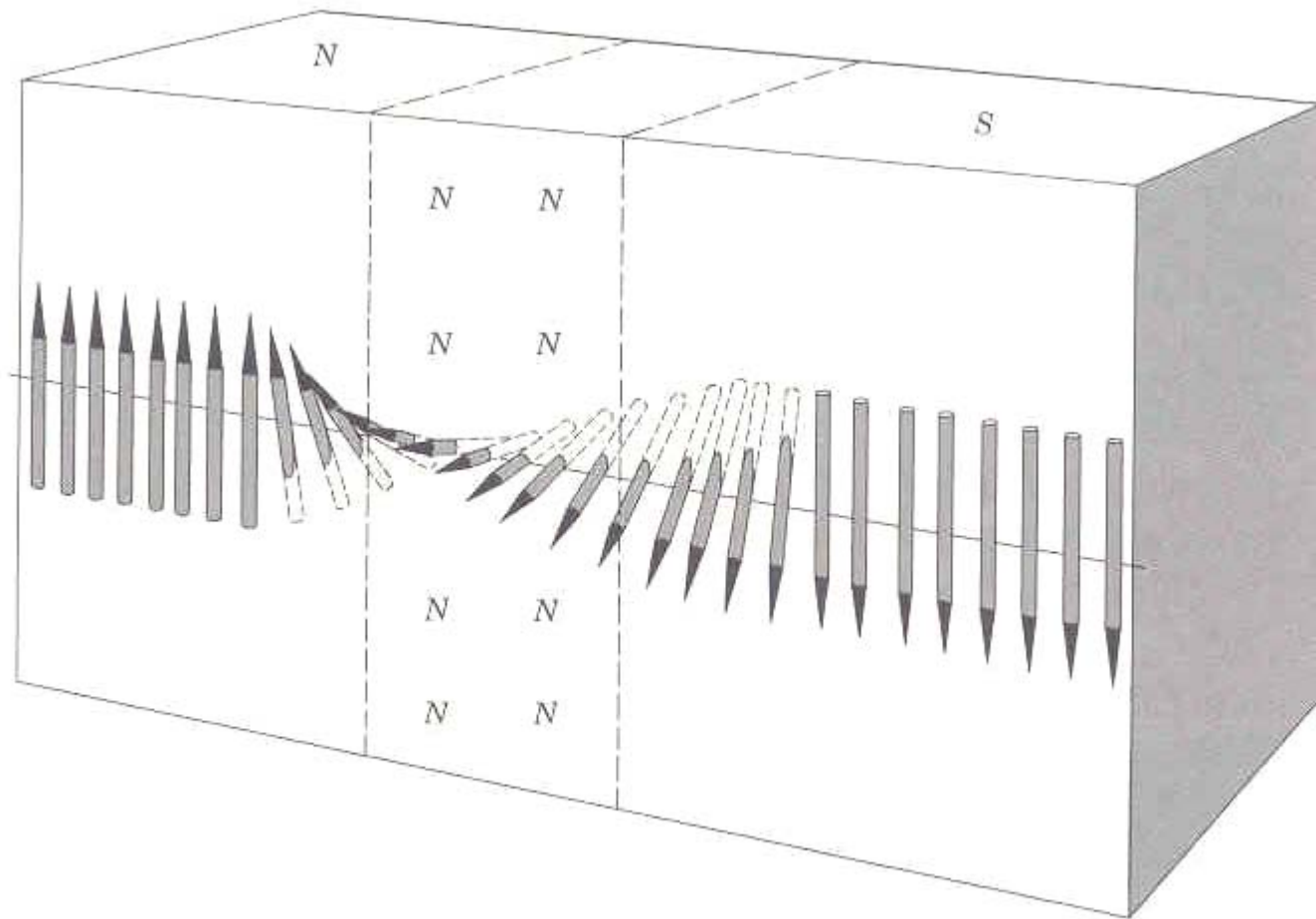
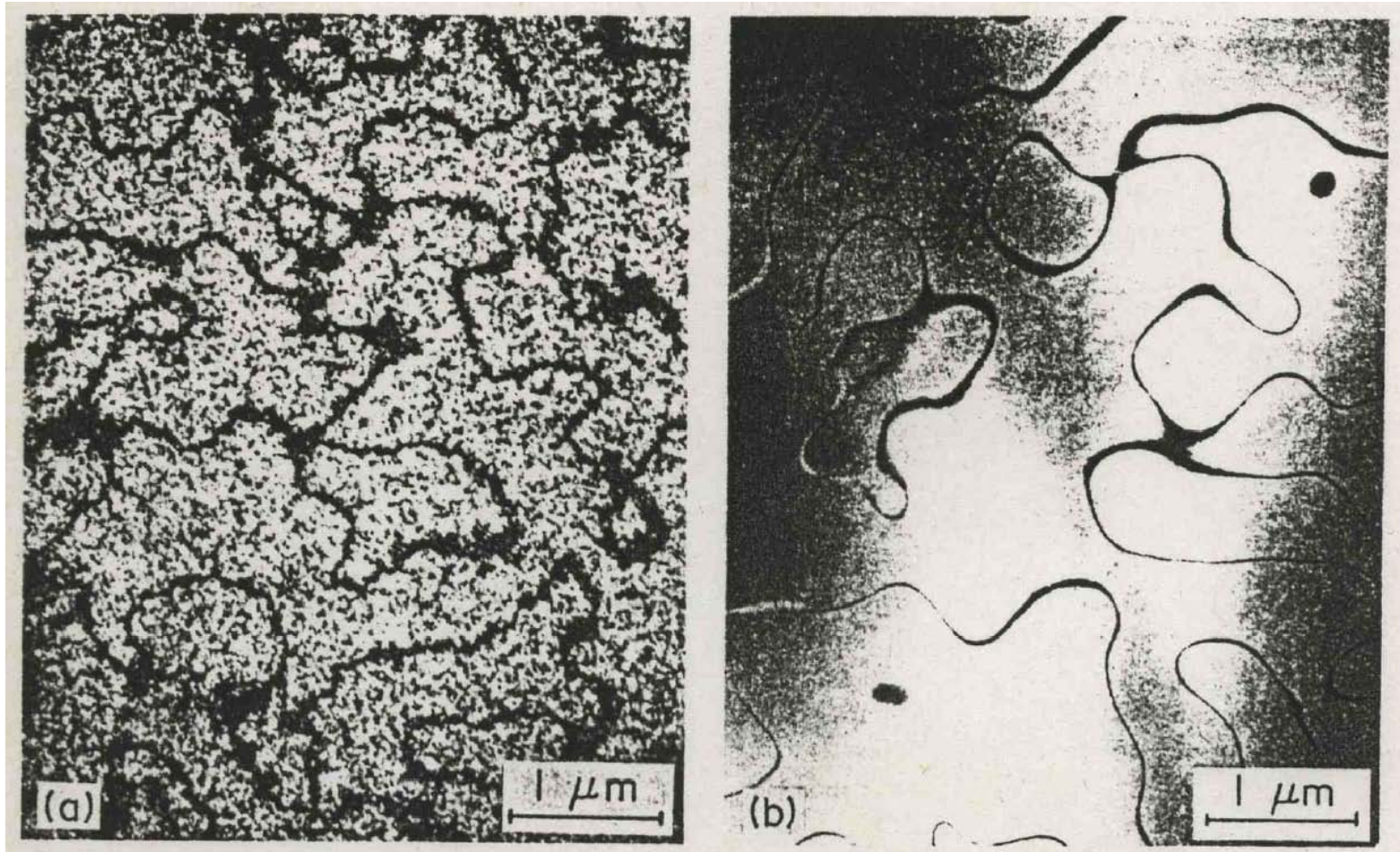


Figure 32 The structure of the Bloch wall separating domains. In iron the thickness of the transition region is about 300 lattice constants.

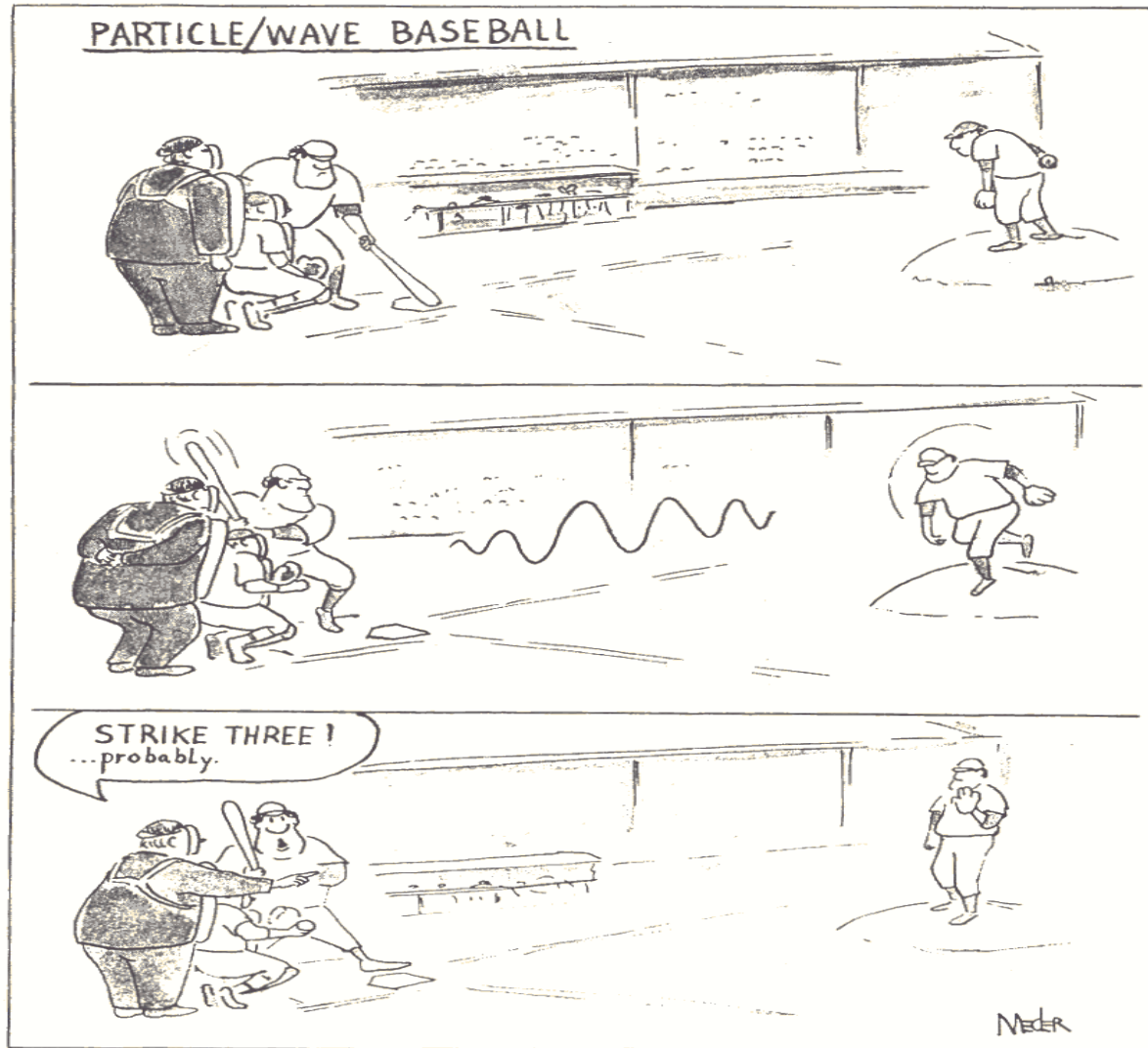
Domain Size (L) vs. Correlation Length of Fluctuations (ξ)



ξ : Correlation Lengths of Fluctuations

L : Domain Size

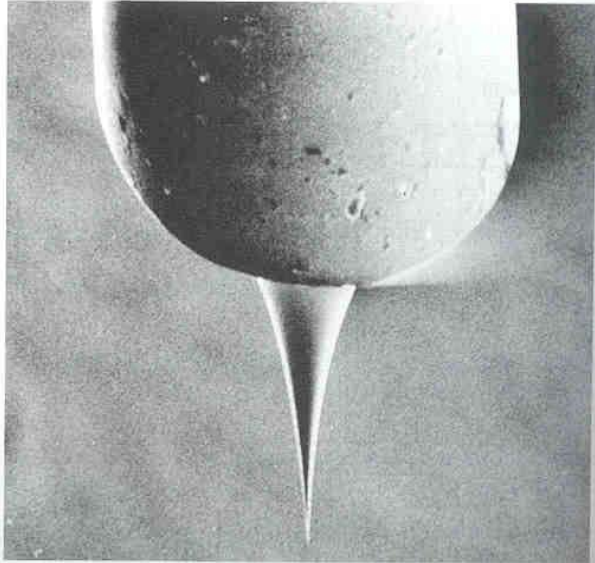
Analysis of Nanomaterials – What Is Going On?



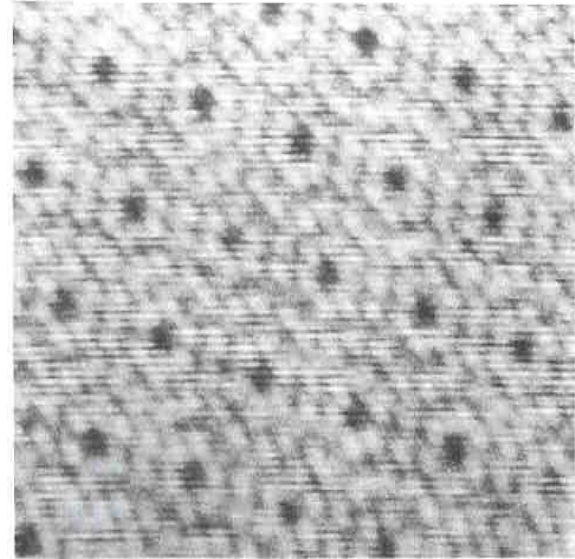
PHYSICS TODAY AUGUST 1990

- 2010-09-08

Scanning Tunneling Microscopy



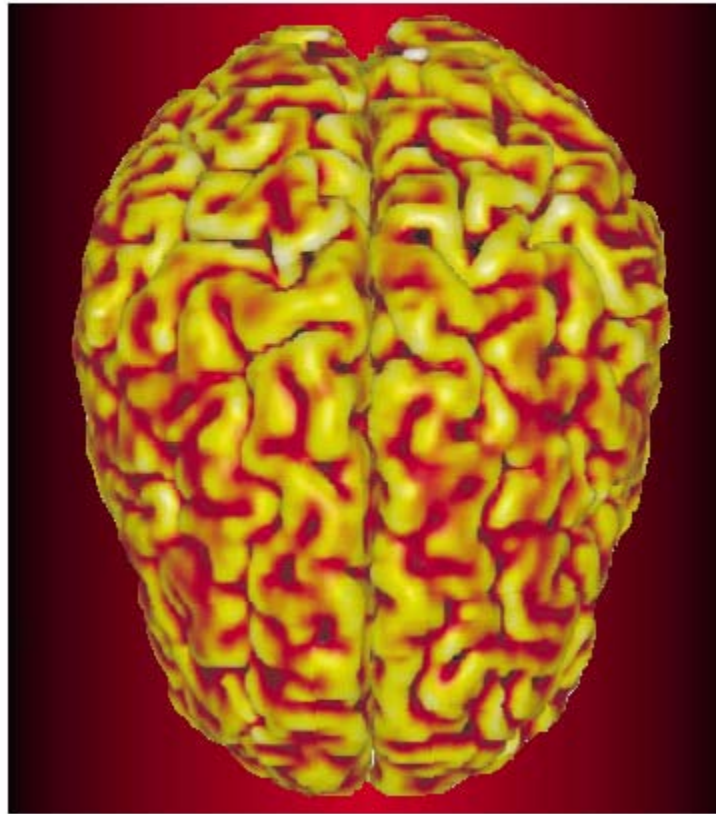
The tungsten probe of a scanning tunneling microscope.



Silicon atoms on Si (111) surface of a silicon single crystal form a repeated pattern (produced by STM).

PHYSICS TODAY

SEPTEMBER 2001



THINK PHYSICS AT NIH

Reconstructing the brain activity from magnetic-resonance imaging.

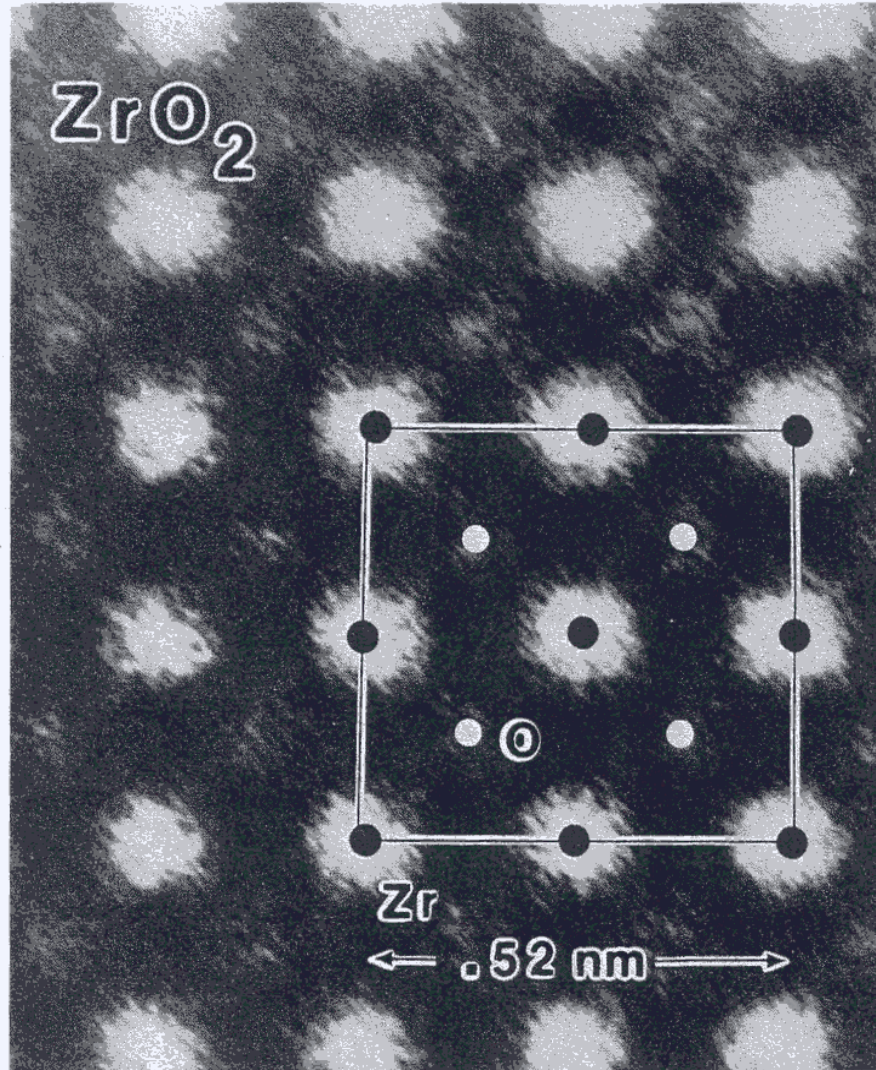
Atomic Hypothesis

If in some cataclysm, all scientific knowledge were to be destroyed, and only one sentence passed on to the next generation of creatures, what statement would contain the most information in the fewest words? I believe it is the atomic hypothesis (or atomic fact, or whatever you wish to call it) that all things are made of atoms.

R. P. Feynman

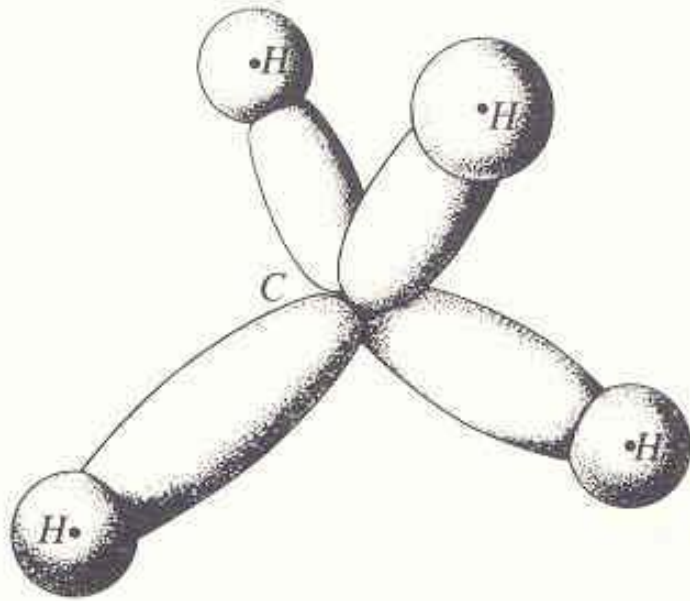
“The Feynman Lectures on Physics”
Addison-Wesley Publishing Company
Reading, Massachusetts
Vol. 1, p. 1–2, 1963

Atomic Arrangement



The atomic-resolution electron microscope permits imaging of the regular arrangement of atoms in a crystalline structure. For this ceramic material, the arrangement of zirconium and oxygen ions can be compared with the atomic-scale geometry of Figure 3.4-3. (Courtesy of R. Gronsky, National Center for Electron Microscopy, Berkeley, California)

Schematic Structure of CH_4 : sp^3 Orbital



sp^3

FIGURE 10

Schematic structure of the methane molecule. The sp^3 orbitals produce bonds arranged like the straight lines joining the center of a tetrahedron to its four corners (angles of $109^\circ 28'$).

Schematic Structure of C_2H_4 : sp^2 Orbital

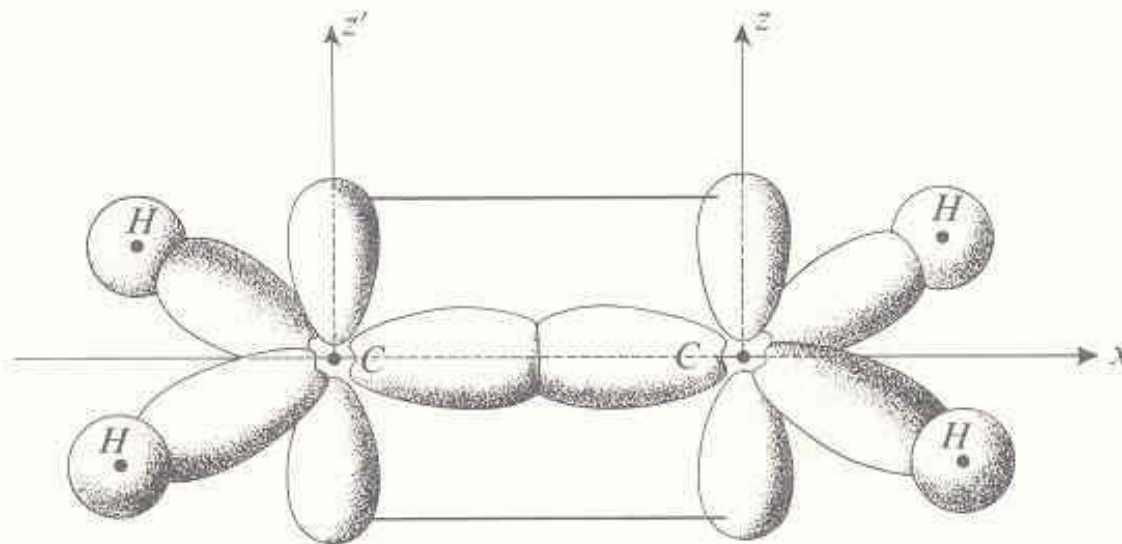
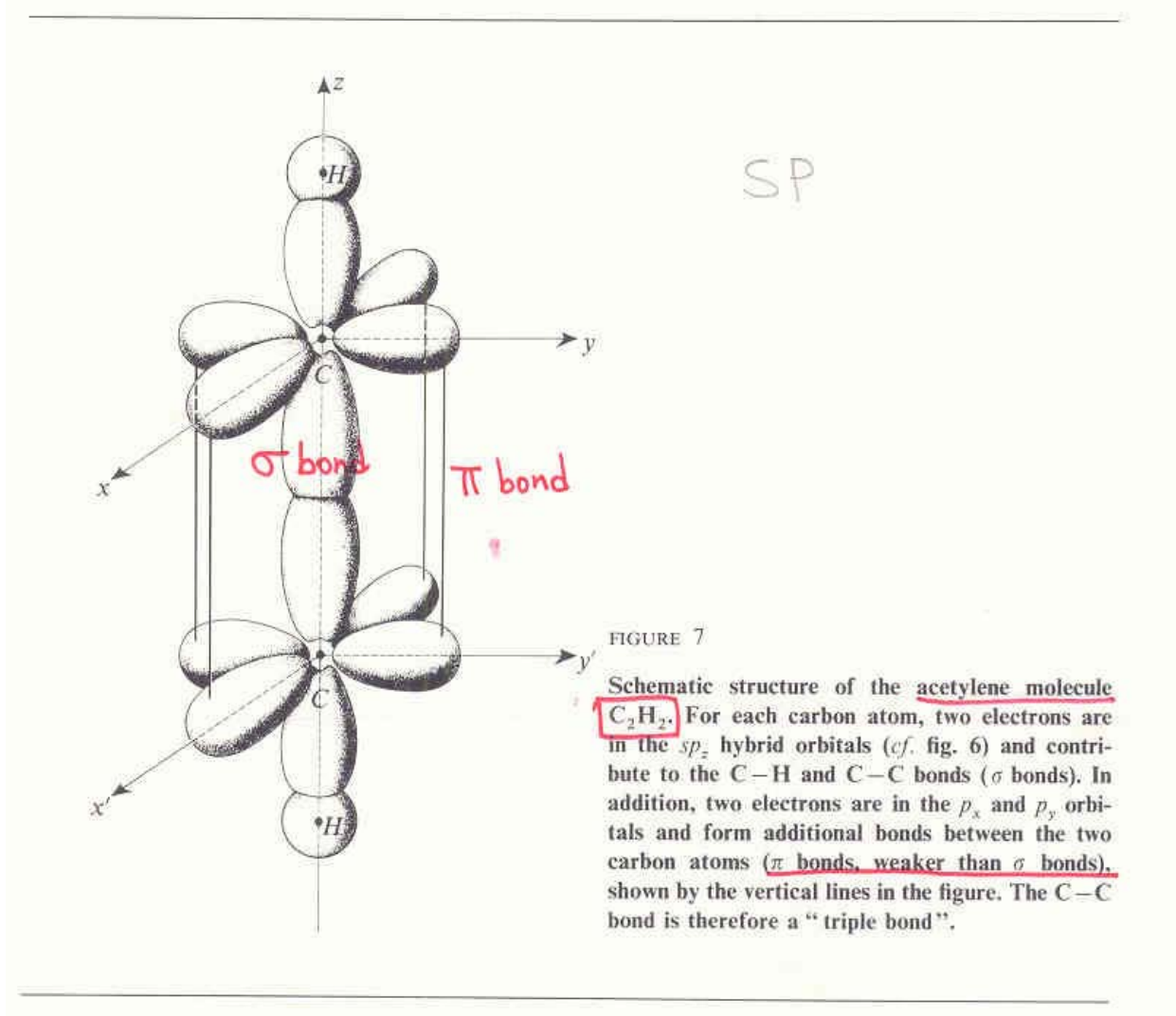


FIGURE 9

Schematic structure of the ethylene molecule C_2H_4 . The two carbon atoms form a double bond with each other : one σ bond due to sp^2 orbitals of the type of those shown in figure 8 (the other two sp^2 hybrid orbitals at 120° with this one form the C - H bonds), and one π bond, due to the overlapping of the p_z orbitals.

Schematic Structure of C_2H_2 : sp Orbital



Icosahedral Crystal (Ga-Mg-Zn)



Fig. 1 Electron diffraction pattern from a $\text{Ga}_{1.0}\text{Mg}_{1.8}\text{Zn}_{2.1}$ icosahedral crystal in a melt-spun ribbon.

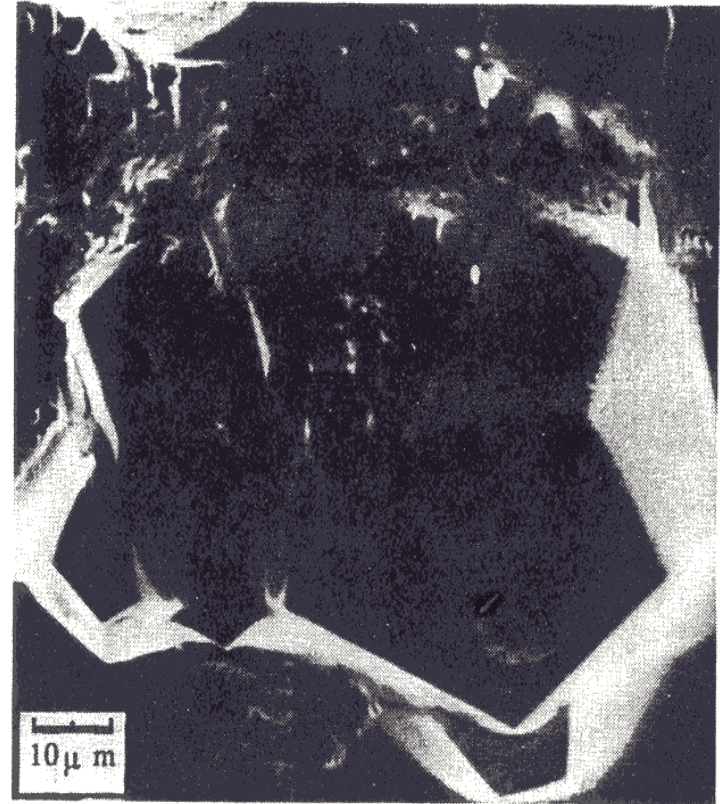
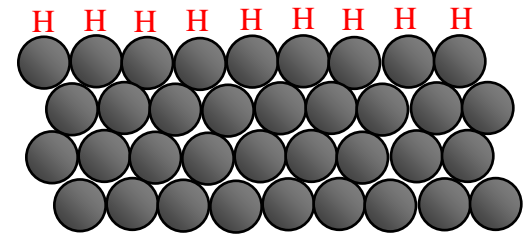
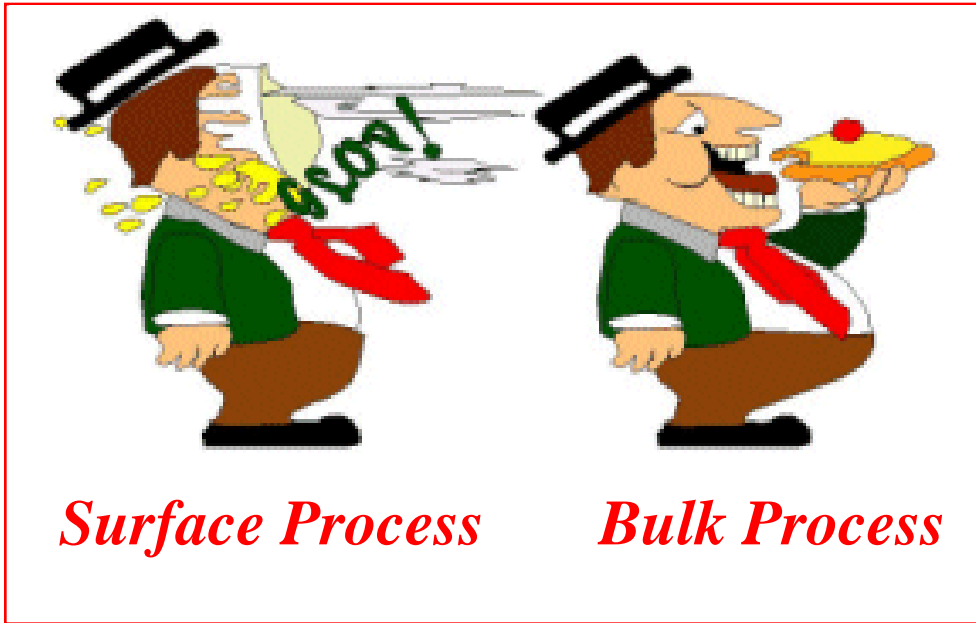


Fig. 3 Scanning electron micrograph of icosahedral crystals with pentagonal dodecahedral growth morphology found in a shrinkage cavity of a slowly cooled $\text{Ga}_{1.0}\text{Mg}_{2.1}\text{Zn}_{3.0}$ ingot.

Adsorption vs. Absorption

Adsorption

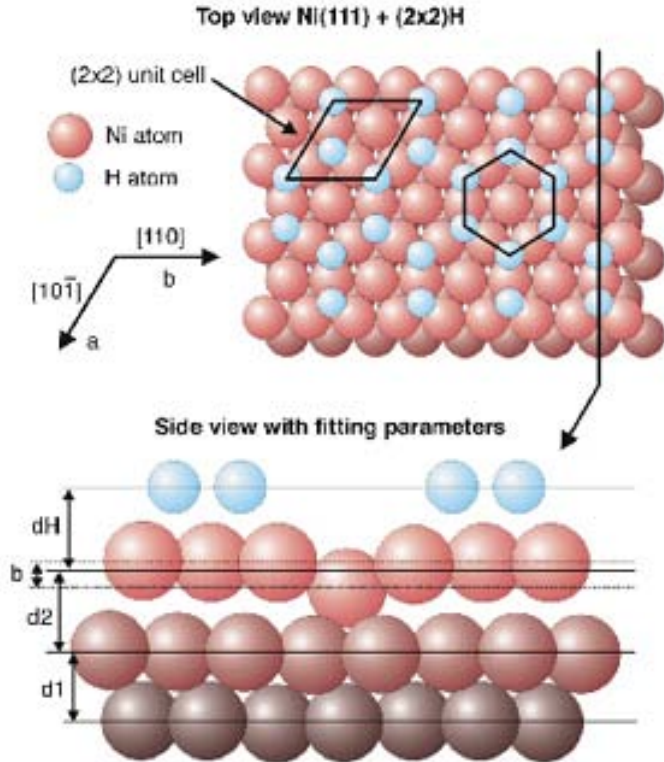
Absorption



H adsorption on Si

Dr. K. L. Yeung (Hong Kong Univ.)
<http://teaching.ust.hk/~ceng511/notes/>

Adsorption vs. Absorption



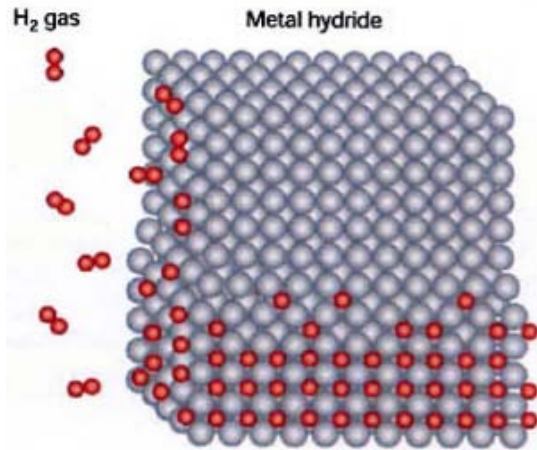
- The model of the UHV low-T p(2×2) structure of H adsorbed on Ni(111) proposed. The fitting parameters of the atomic model are shown.
- The values of these parameters found from our SXRD data compare well with the ones found from the LEED study.
- K. Müller's group (Universität Erlangen-Nürnberg, Germany)
Phys. Rev. B **47**, 15969 (1993)

Hydrogen-induced restructuring of close-packed metal surfaces: H/Ni(111) and H/Fe(110)

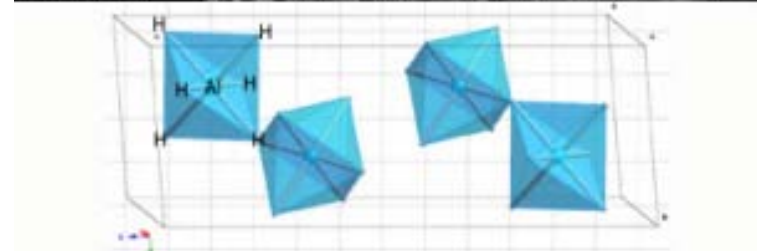
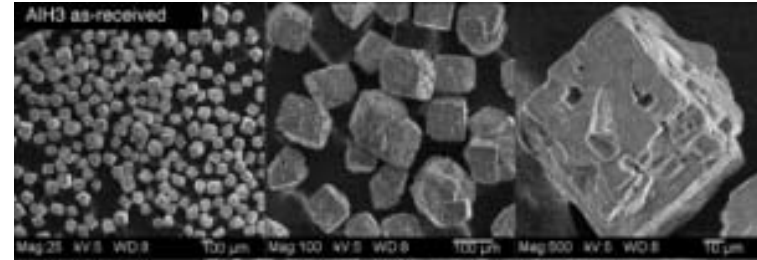
L. Hammer, H. Landskron, W. Nichtl-Pecher, A. Fricke, K. Heinz, and K. Müller
Festkörperphysik, Universität Erlangen-Nürnberg, Staudt-Strasse 7, D-8520 Erlangen, Germany
(Received 4 March 1993)

We report that hydrogen can induce surface reconstructions by adsorption even on close-packed substrates. New low-energy electron-diffraction analyses for H/Ni(111) and H/Fe(110) show that consideration of reconstruction is essential for a convincing experiment-theory fit as well as for reliable determination of the adsorption site. There are two different types of reconstruction: Hydrogen pulls nickel atoms out of the surface but pushes iron atoms towards the bulk. These findings are mirrored by a different sign of work-function change for both systems and demonstrate the correlation between geometric and electronic structure.

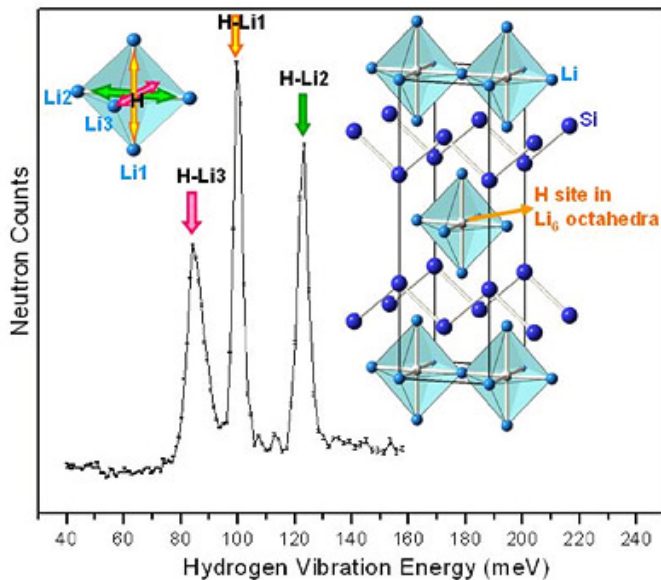
Metal Hydride – Hydrogen Storage



Schematic of Metal Hydride
from MRS Bulletin **27** (2002)



SEM and Crystal Structure of **AlH₃**
DOW Chem. Co.
<http://www.dow.com>



Structure and Vibration of Hydrogen Atoms bound in **Li₄Si₂H**
University of Maryland
<http://www.mse.umd.edu/research/spotlight/h-storage.html>

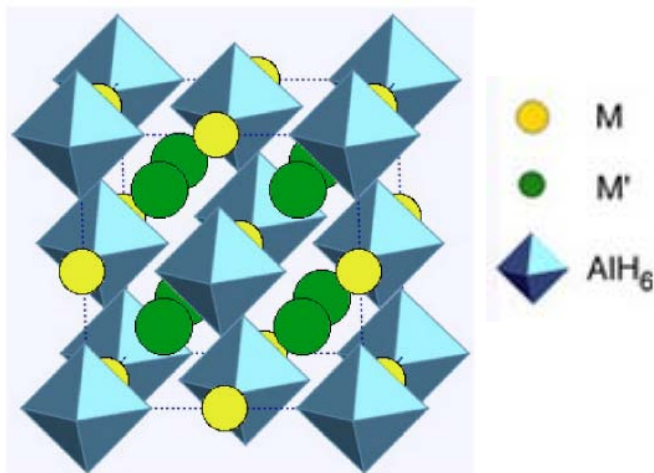


FIG. 7. (Color online) Structural diagram of $M_2M'AlH_6$ showing AlH_6 octahedra, M cations (large) and M' cations (small).

J. Graetz *et al.*

Phys. Rev. B **71**, 184115 (2005)

PHYSICAL REVIEW B 71, 184115 (2005)

Structures and thermodynamics of the mixed alkali alanates

J. Graetz,¹ Y. Lee,² J. J. Reilly,¹ S. Park,² and T. Vogt²

¹*Department of Energy Sciences and Technology, Brookhaven National Laboratory, Upton, New York 11973, USA*

²*Department of Physics, Brookhaven National Laboratory, Upton, New York 11973, USA*

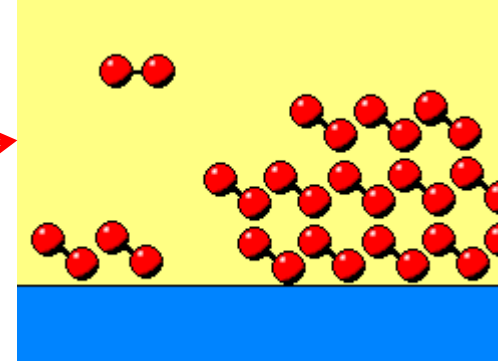
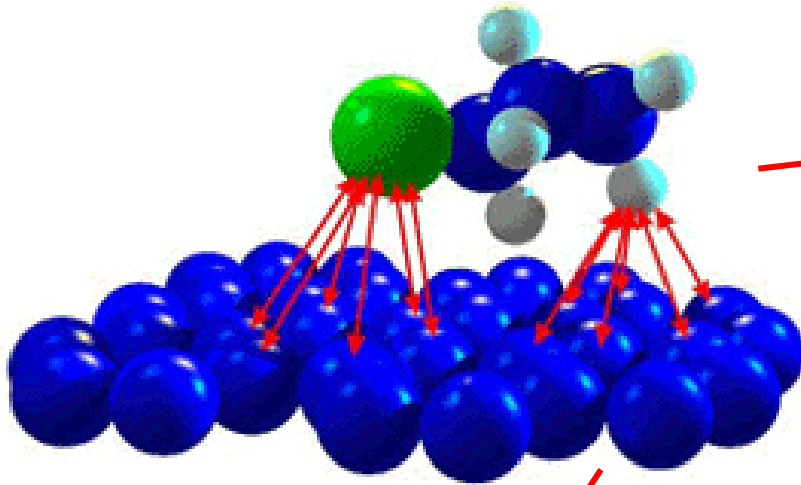
(Received 20 January 2005; revised manuscript received 10 March 2005; published 27 May 2005)

The thermodynamics and structural properties of the hexahydride alanates ($M_2M'AlH_6$) with the elpasolite structure have been investigated. A series of mixed alkali alanates (Na_2LiAlH_6 , K_2LiAlH_6 , and K_2NaAlH_6) were synthesized and found to reversibly absorb and desorb hydrogen without the need for a catalyst. Pressure-composition isotherms were measured to investigate the thermodynamics of the absorption and desorption reactions with hydrogen. Isotherms for catalyzed (4 mol% $TiCl_3$) and uncatalyzed Na_2LiAlH_6 exhibited an increase in kinetics, but no change in the bulk thermodynamics with the addition of a dopant. A structural analysis using synchrotron x-ray diffraction showed that these compounds favor the $Fm\bar{3}m$ space group with the smaller ion (M') occupying an octahedral site. These results demonstrate that appropriate cation substitutions can be used to stabilize or destabilize the material and may provide an avenue to improving the unfavorable thermodynamics of a number of materials with promising gravimetric hydrogen densities.

DOI: 10.1103/PhysRevB.71.184115

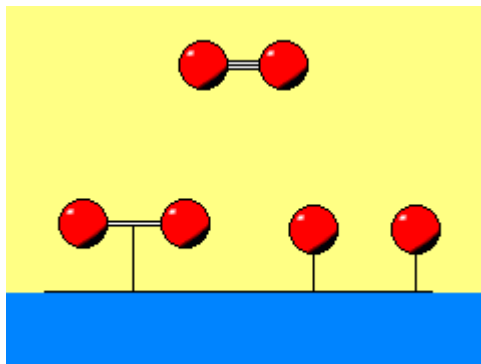
PACS number(s): 82.60.-s, 61.10.Nz, 61.66.Fn, 82.60.-s

Types of Adsorption Modes



Physical Adsorption or Physisorption

Bonding between molecules and surface is by weak van der Waals forces.



Chemical bond is formed between molecules and surface.

Chemical Adsorption or Chemisorption

Dr. K. L. Yeung (Hong Kong Univ.)
<http://teaching.ust.hk/~ceng511/notes/>

나노산업기술연구조합 | 17937-90 서울시 서초구 우면동 69-2 세신우면중환상가 301호 | ☎ 02-2057-8507-8 | 02-2057-8509 | E. nanokorea@nanokorea.net

기획기사 | Special Report

나노 융합기술 R&D 및 산업화



컬럼 | Column

나노산업 강국을 기대하며...

(서울대학교 환민구 교수)

인사이드 인터뷰 | INSIDE Interview

나노산업의 철병, 나노소재 산업

(KIST 박종구 본부장)

정책동향

2008년도 나노기술발전 시행계획

조합소식

산업탐방 / 회원사 동향 / 사무국 일정 · 행사

나노라이프

美 "NSTI nanotech 2008"

Conference & Trade Show 참관기

미리보는 행사

나노코리아 2008

MRS Spring Meeting



Mountaineering



House Party



Covalent Bonding

